Development of an Adaptive Polarization-Mode Dispersion Compensation System

by

Arun-Prasad Chimata

B.E. (Electrical and Electronics Engineering), University of Madras, Chennai, India, 2000

Submitted to the Department of Electrical Engineering and Computer Science and the Faculty of the Graduate School of the University of Kansas in partial fulfillment of the requirements for the degree of Master of Science.

_____
Professor in charge

_____

_____
Committee members

_____
Date thesis accepted

Abstract

Polarization-mode dispersion (PMD), in single-mode optical fibers, is a phenomenon that can limit the bit-rate-distance product of amplified, lightwave communication systems. PMD compensation is a solution to overcome the limitations posed by PMD. However, compensation is complicated due to the random nature of PMD. Therefore, adaptive compensation techniques are required.

We modified an adaptive PMD compensation system that was earlier developed and made it robust and bit-rate independent. The new set-up uses the degree of polarization (DOP) of the received optical signal for monitoring the fiber-link's PMD. An analog voltage equivalent of the DOP, commonly referred to as the PMD monitor signal, is used for the PMD compensation. We performed experiments to identify the effect of polarization scrambling on the PMD monitor signal and to find the appropriate range of scrambling frequencies. The appropriate polarization scrambling frequency range for the present set-up was determined to be between 80 Hz and 100 Hz.

Next, we performed different tests on the adaptive PMD compensation system. The time taken by the compensator to complete a compensation cycle was determined to be 100 s. OSNR (optical signal to noise ratio) tests were conducted from which it was determined that the PMD compensator could perform satisfactory compensation at 10 dB of OSNR and above. We then successfully performed a field trial of the adaptive PMD compensation system on an underground fiber-optic link spanning about 95 km.

Acknowledgements

I wish to express my sincere gratitude to Dr. Chris Allen for providing me the opportunity to work with him in the lightwave communication systems laboratory. I would like to thank him for his guidance, encouragement and countless contributions for my education and research endeavors in the University of Kansas.

I would like to thank Dr. Ron Hui, Dr. Ken Demarest and the Sprint Corporation for their contributions to my learning and for participating in my research work. I would like to thank Dr. Hui for helping with the power budget calculation.

I would like to thank Juan Madrid for sharing his knowledge about the PMD compensation system and for his support. Juan developed the PMD compensation program and designed and built the interface board, in addition to other things.

I would like to thank my former and present colleagues in the lightwave laboratory for their support and cooperation. Renxiang Huang (Ray) designed the voltage inversion and scaling circuit.

I would like to thank my family members, well-wishers, friends and GOD for their love and encouragement, without which nothing would have been possible.

Table of contents

List of figures

Chapter 1

Chapter 2

List of tables

Chapter 4

1. INTRODUCTION

The growth of telecommunication technologies has been phenomenal since the past century and a half. From the early telegraph to the present day high speed optical systems, there has been a constant upward surge in the data rates and the system capabilities. Figure 1.1 shows the increase in the bit-rate-distance product since 1850.

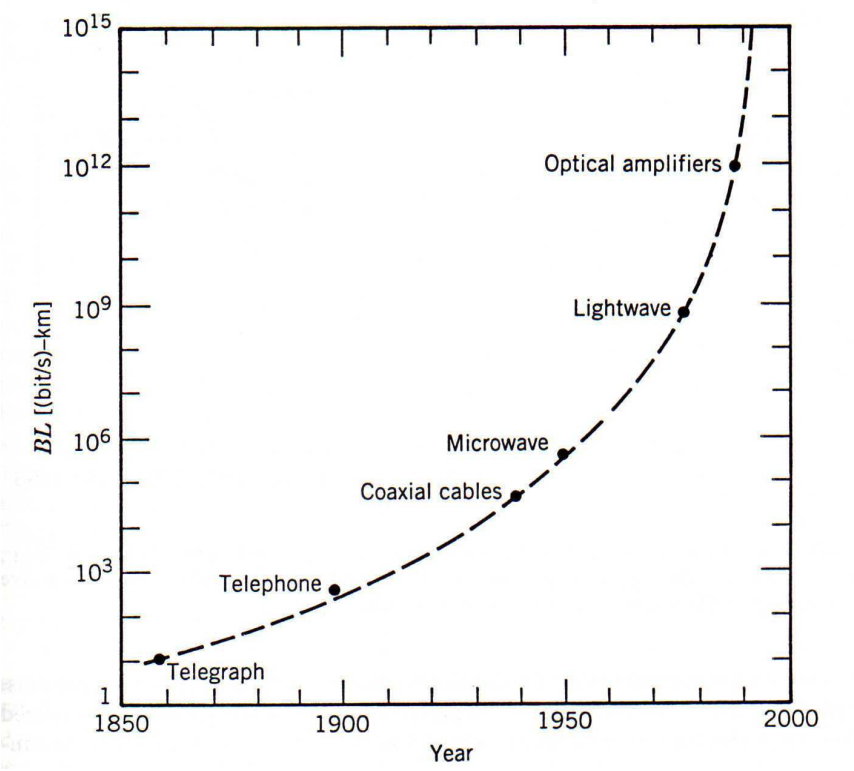

Figure 1.1 Increase in the bit rate –distance (B-L) product since 1850 [1]

The feasibility of using glass fiber for optical communication was seriously studied in the mid-1960s. Dr. Charles Kao and others proposed that it would be possible to reduce fiber attenuation to less than 20 dB/km. In 1970, Corning Incorporated actually developed a single-mode fiber which had a loss

of less than 20 dB/km at an operating wavelength of 633 nm (helium-neon line). Since then, several advancements enabled optical fiber communication to become practical and feasible. Figure 1.2 depicts the growth of fiber-optic systems since 1974.

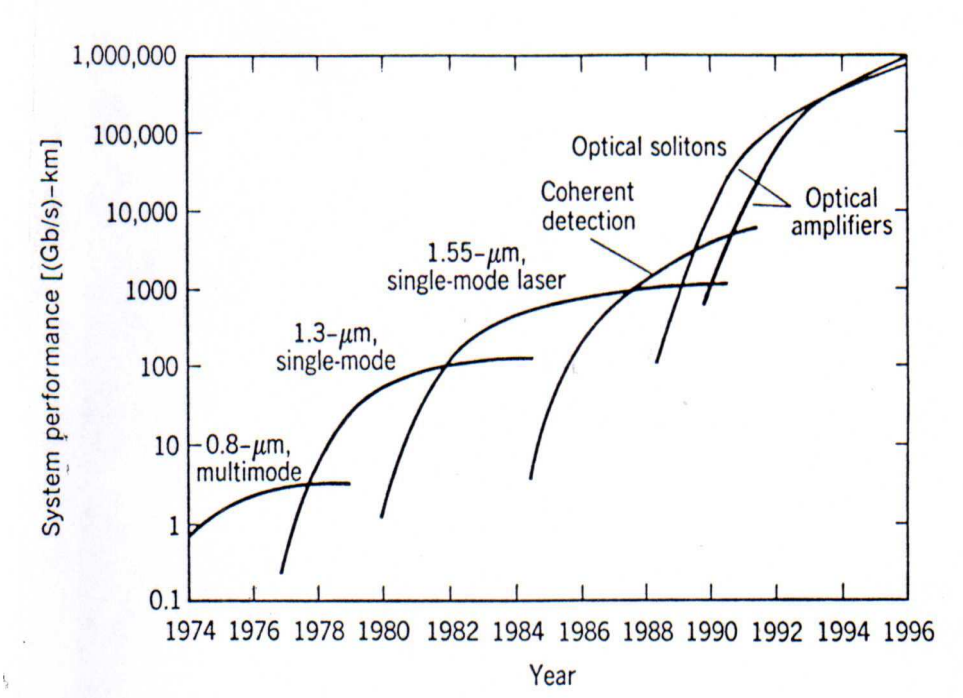

Figure 1.2 Progress in optical fiber communication since 1974 [1]

The mid 1980s saw telecommunication carriers like Sprint establish extensive fiber optic backbone networks. And with the advent of the optical amplifier, or specifically the Erbium Doped Fiber Amplifier (EDFA) in 1986, it has been possible to increase the span and speed of optical fiber based communication systems. The EDFA band, or the range of wavelengths over which the EDFA can operate, proved to be an important factor in fixing the wavelength of operation of present day fiber optic systems. The EDFA band

is wide enough to support many wavelengths simultaneously. This led to the development of Wavelength Division Multiplexed (WDM) systems or the simultaneous propagation of several wavelengths of light through a fiber. Each wavelength can carry a different data stream.

In the 1990s, the demand for bandwidth, especially with the growth of the internet, fueled a rapid increase in the data rates. As the number of channels and data rates rose, certain phenomena such as chromatic dispersion and non-linearities began to show up as obstacles. Chromatic dispersion, being deterministic in nature, could be effectively compensated for by using special fibers called dispersion compensating fibers and other novel devices. Non-linearities could also be minimized with careful power budget consideration. With all these measures, the upward surge of the data rate would have seemed unstoppable. However, at very high data rates (above 10 Gb/s) even minute phenomena have to be taken into consideration to ensure error-free transmission. Examples of such phenomena are polarization-dependent broadening and polarization-dependent loss of the optical signal. The optical fiber has some inherent properties like birefringence, which leads to what is called polarization-mode dispersion (PMD). The following paragraphs will provide the definition of PMD and will discuss why PMD plays an important role in the design of high speed fiber-optic telecommunication systems.

1.1 Definition of PMD

A single-mode fiber is designed to support only one mode of propagation of light. The principal advantage of letting light propagate along only one mode is that inter-modal dispersion can be avoided. Inter-modal dispersion happens as a result of relative delay between the light propagating in the various modes in a multi-mode fiber. In single-mode fibers, as there is only one mode available for light propagation (theoretically), inter-modal dispersion is non-existent.

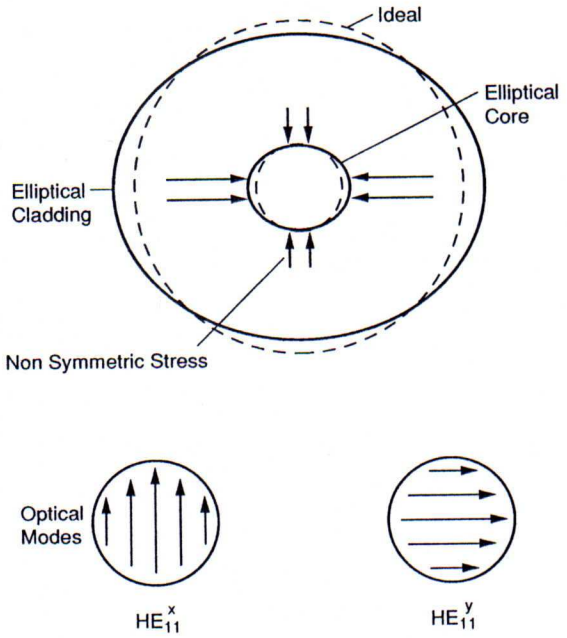

Figure 1.3 Stresses and modes in a single mode fiber [2]

In reality, however, there are two modes of propagation of light even through a single-mode fiber. In spite of the measures taken to provide a symmetrical core cross-section, there is some asymmetry. (Figure 1.3 illustrates how stress can induce asymmetry in the fiber core). The consequence of this asymmetry

of core cross-section is the existence of birefringence. As a result, when a light pulse is input into a fiber core, it is decomposed into two orthogonally polarized components that propagate with different propagation characteristics. The pulses arrive at the output differentially delayed. This difference between the delays is termed as the differential group delay (DGD). It is this DGD that causes an input pulse to appear broadened at the output. And this effect on the pulse is commonly called PMD.

1.2 What causes PMD?

The reasons for birefringence in single mode fiber can be broadly classified as intrinsic and extrinsic. Intrinsic factors are those that are present in the fiber right from the manufacturing stage. When specialized methods had not evolved, the fiber drawing process induced some asymmetry that caused birefringence. Fibers thus manufactured (sometimes referred to as legacy fibers) can have rather high levels of PMD (0.5 ps/√km or greater). Present day fibers are manufactured with extra care and thus minimal asymmetry results. PMD levels are typically < 0.1 ps/√km for such fibers. Extrinsic factors are those which induce birefringence in a fiber after it's manufacture. Cabling of fiber after it's manufacture can cause stresses that induce birefringence. External pressure can also induce birefringence in a fiber (e.g. bending). There have been reports about the influence of temperature on fiber's birefringence too [2].

1.3 Effects of PMD in fiber-optic systems

The effects of birefringence and PMD are considered differently for short, single-mode fiber spans and long, single-mode fiber spans. All telecommunication fibers fall in the "long" fiber category. But still, understanding the PMD mechanism in "short" fibers would help explain the mechanisms in the "long" fibers.

In a short fiber segment, the stresses can be considered to be acting uniformly along the length. The single-mode fiber segment becomes bi-modal due to the birefringence induced by these stresses. The propagation constants along the two (propagating) modes are slightly different. Therefore, a differential delay develops in the fiber segment, which is capable of broadening an input pulse. Mathematically, this broadening can be described as follows:[2]

If β_s and β_f are the propagation constants along the slow and fast propagation modes respectively and if n_s and n_f are their effective refractive indices, then:

$$\beta_s - \beta_f = \frac{\omega n_s - \omega n_f}{c} = \frac{\omega \Delta n}{c} \qquad (1.1)$$

where, ω and c are the angular frequency of the light signal and free-space velocity of light, respectively. The differential group velocity, expressed as group delay per unit length is obtained from (1.1) by taking the frequency derivative of the propagation constants [2].

$$\frac{\Delta\tau}{L} = \frac{d}{d\omega}(\beta_s - \beta_f) = \frac{\Delta n}{c} - \frac{\omega}{c}\frac{d\Delta n}{d\omega} \qquad (1.2)$$

The group delay per unit length term $\frac{\Delta\tau}{L}$ is commonly known as the PMD coefficient of a fiber. It's unit is ps/km. Figure 1.4 illustrates the effect of birefringence on a pulse input into a short fiber segment.

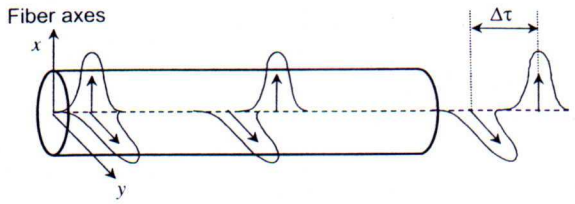

Figure 1.4 A pulse launched with equal power on the two birefringent axes x and y of a short fiber segment gets separated by the DGD ($\Delta\tau$) at the output [5]

As mentioned earlier, since all telecommunication grade fibers fall in the "long" fiber category, it is necessary to bring out their differences from the "short" fibers. The relation between PMD induced delay and fiber length is no longer linear in the case of long fibers. This is because of the phenomenon called mode coupling that is taking place in all fibers longer than a certain statistical length called correlation length or coupling length. Fibers that are shorter than the correlation length are considered to belong to the "short" fiber category and all the other fibers are considered to belong to the "long" fiber category. As a lightwave propagates down a fiber, there is a constant sharing of energies between the two propagating modes. This random exchange of energies is due to the varying stresses or perturbations that are experienced by the fiber along it's length.

In order to define the correlation length, let us assume that a lightwave signal is input into a fiber, aligned to a certain polarization mode. The correlation length is a statistical quantity defined as the length at which the average power in the orthogonal polarization mode (the mode perpendicular to the input mode) is within $\frac{1}{e^2}$ of the power in the input mode [2]. The correlation length can vary between a few meters to more than a kilometer depending on whether it is a spooled fiber or a cabled fiber. Telecommunication grade fibers will typically have a value of 100 m [3].

The effect of mode coupling is that the DGD has a square root of length dependence rather than a linear length dependence. However, in either case, PMD causes dispersion or broadening of the lightwave signal. Whereas this broadening is predictable in the case of short length fibers, it is probabilistic for long length fibers.

In digital fiber-optic systems, the PMD effects can be assessed by estimating the power penalty incurred. The expression for the PMD induced power penalty is [2]:

$$\varepsilon \cong A\frac{\Delta\tau^2\gamma(1-\gamma)}{T^2} \tag{1.3}$$

where, ε is the power penalty in dB, $\Delta\tau$ is the DGD, γ is the power splitting ratio between the two component modes ($0 \leq \gamma \leq 1$), T is the full-width at

half maximum of the lightwave pulse. The factor *A* is a dimensionless parameter determined by the pulse shape and receiver characteristics. Another relation that gives an estimate of the PMD induced limitation on the bit rate and the span of a digital fiber-optic system is [2]:

$$B^2 L \approx \frac{0.02}{(PMD)^2} \tag{1.4}$$

where, B and L are the bit-rate (Gb/s) and link length (km), respectively, and PMD has the units of ps/√km. This relation was arrived at by considering the case that the PMD induced delay must be less than 14% of the bit period in order to avoid incurring PMD-induced power penalty of 1 dB or greater for a period of 30 min per year [2]. Figure 1.5 shows the bit error fluctuations due to the variable nature of PMD and the influence of temperature on it's variability.

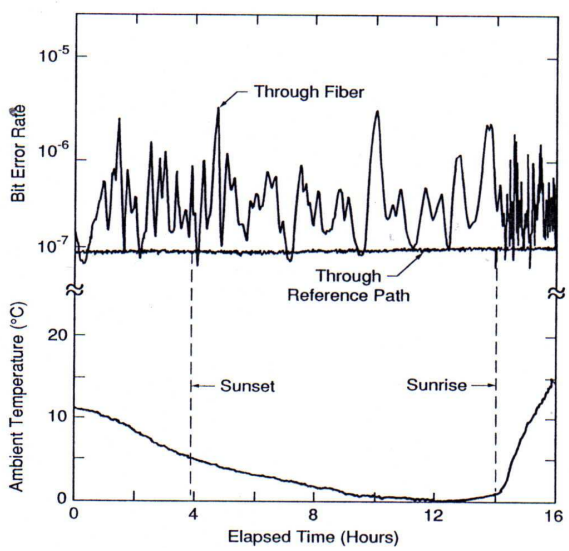

Figure 1.5 Measured bit error rate fluctuations due to PMD in a digital fiber optic system. The rate of ambient temperature change appears to change the rate of the fluctuations. [2]

1.4 Characterization of PMD

PMD in telecommunication fibers is a stochastic or random process. Therefore the penalties due to PMD are also random. In order to develop effective compensation techniques it is necessary to understand the nature and characteristics of PMD.

1.4.1 The PSP concept

In order to satisfactorily understand and explain the observed statistical effects associated with PMD, models have been proposed. One model is the coupled-power model (low coherence model) for long fiber spans. This model was originally developed for multi-mode fibers. However, the most prominent among the models, which is best suited for modeling long single mode fibers, is the principal states model (high coherence model) [2,4]. According to the principal states model, a single-mode fiber can be thought to have a set of two orthogonal principal states of polarization (PSPs) which have certain properties as described below. A light pulse aligned with one of the fiber's two input PSPs will emerge out of the fiber end as a single pulse, unchanged in shape. Also, the emerging pulse will be polarized along the corresponding output PSP of the fiber. On the other hand, if the pulse's state of polarization (SOP) is aligned anywhere between the two input PSPs (but not aligned along either of them), the pulse will be split into two orthogonal components. Moreover, due to the differential group delay, or DGD, these components will arrive at the output at different times, resulting in pulse broadening. Based on

this PSP concept, a long single-mode fiber may be modeled as a concatenation of randomly oriented, short sections of birefringent fiber [2]. Figure 1.6 compares the pulse splitting in the low coherence model with that in the high coherence model.

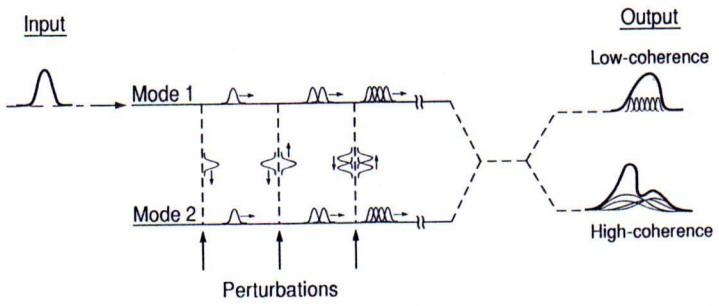

Figure 1.6 Comparison of low coherence and high coherence concepts [2]

The frequency domain definition of PSP can be described as follows [5]. For a length of fiber, at every frequency, there is a pair of input polarization states called the PSPs. A PSP is that input polarization state for which the output state of polarization is independent of frequency over a small frequency range. Using the PSP concept, PMD can be characterized as a vector represented as [5]:

$$\vec{\tau} = \Delta\tau\, \hat{p} \tag{1.5}$$

The PMD vector is a vector in three dimensional space (Stokes space). The length of the vector ($\Delta\tau$) is the DGD and the direction of the vector ($\hat{p}$) is along the axis that joins the two output PSP points in Stokes space [4,5]. Any input state of polarization (SOP) can be expressed as the vector sum of two components, each component being aligned with one of the PSPs. For a

narrow band source (i.e., considering only first-order PMD) the output electric field vector from a fiber can be given as [2,6]:

$$\vec{E}_{out}(t) = c_{+}\hat{p}_{+}.\vec{E}_{in}(t+\tau_{+}) + c_{-}\hat{p}_{-}.\vec{E}_{in}(t+\tau_{-}) \qquad (1.6)$$

where, $\vec{E}_{out}(t)$ and $\vec{E}_{in}(t)$ are the output and input electric field vectors respectively. c_{+} and c_{-} are complex coefficients required to indicate the field amplitude launched along the slow PSP and fast PSP respectively. The magnitudes, $|c_{+}|$ and $|c_{-}|$, correspond to the power splitting ratio γ, seen in (1.3). $\hat{p}_{+}$ and $\hat{p}_{-}$ are unit vectors specifying the output polarization states (referred to as output PSPs) of the two components. The difference $(\tau_{+}\text{-}\tau_{-})$ is $\Delta\tau$, the DGD. This relation shows that the amount of broadening of the output pulse due to PMD is dependent upon the values of the quantities $\Delta\tau$, c_{+} and c_{-} [2,6]. Figure 1.7 shows the observed time delay between pulse components along the two PSPs.

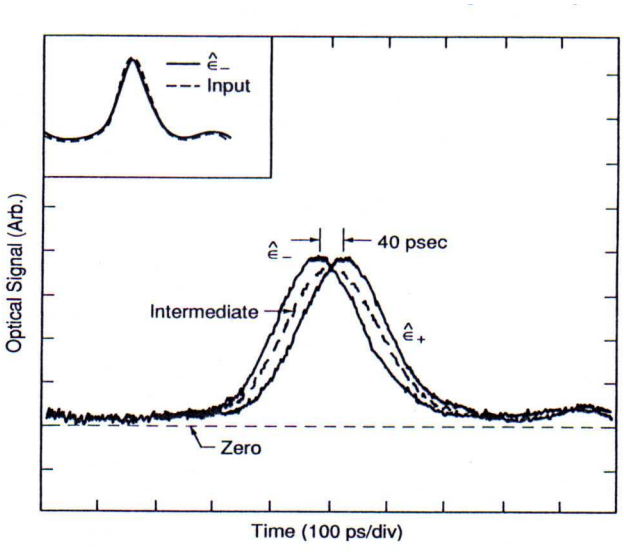

Figure 1.7 Measured DGD between pulse components along the two PSPs [2, 6]

1.4.2 PMD statistics

The PSP model has facilitated the investigation of the statistical properties of PMD. It is now a well established fact that the average DGD has a square root of length dependence. The probability density function of DGD is Maxwellian over time and over wavelength. Figure 1.8 illustrates how the plot of measured DGD closely matches that of a Maxwellian function.

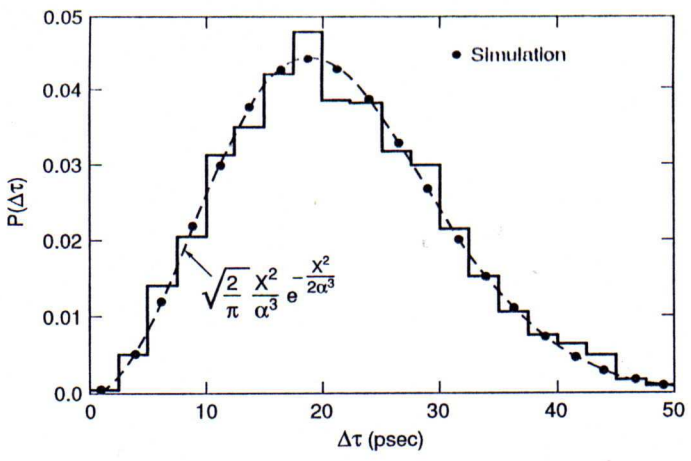

Figure 1.8 The measured probability density function of DGD and the Maxwellian fit (dotted line) [2]

1.4.3 Higher order PMD

Among all the higher orders, it is the second-order PMD that has been attached the most significance and thereby there is considerable amount of literature existing on it. The discussion here will be limited to second-order PMD. The PMD vector, owing to it's dependence on the angular frequency ω, can be expanded as a Taylor's series with ω as the independent variable. The

second order term in the expansion corresponds to second order PMD. Second order PMD can be described by the derivative [5]:

$$\vec{\tau}_{\omega} = \frac{d\vec{\tau}}{d\omega} = \Delta\tau_{\omega}\,\hat{p} + \Delta\tau\,\hat{p}_{\omega} \tag{1.7}$$

where, the subscripted variables are derivatives with respect to the subscript. The physical significance of second-order PMD is that it causes a polarization- dependent pulse broadening or compression (termed as polarization dependent chromatic depression or PCD) and a depolarization of PSPs or the rotation of the PSPs with frequency. The first term on the right side of (1.7) represents PCD and the second term represents PSP depolarization. The magnitude of the first term $\Delta\tau_{\omega}$ (the PCD term) is the change in DGD with frequency. The magnitude $|\hat{p}_{\omega}|$ represents the rate of angular rotation of the PMD vector [5]. The units are ps/nm for the PCD term and ps for the PSP depolarization term. Figure 1.9 is a plot showing the change in DGD over a range of 20 nm.

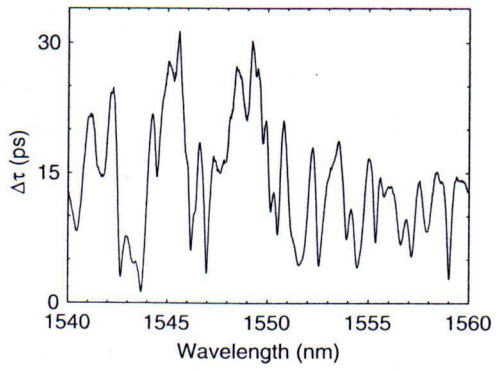

Figure 1.9 DGD plotted as a function of wavelength [5]

2. PMD MITIGATION

2.1 Introduction

As explained in the previous chapter, PMD can cause several undesirable effects that could be obstacles to high speed telecommunication through optical fibers. Such effects are not limited to digital communication systems but affect analog communication systems as well [7].

With the evolution of specialized manufacturing methods, PMD in present day, telecommunication grade fibers is kept very low (< 0.1ps/√km). Still, no matter how good the fiber may be, at some bit-rate-length product, PMD will be an issue. Hence, there is need to investigate strategies for PMD mitigation.

Over the years, research groups from around the globe have proposed and/or demonstrated different strategies for PMD compensation. In this chapter an overview of these strategies shall be given. Their relative merits and demerits will also be mentioned. Following that, methods to increase the tolerance of a fiber-optic communication system to PMD, will also be discussed.

2.2 PMD compensation strategies

The more widely researched PMD compensation techniques are summarized in section 2.2.1, followed by a summary of other techniques.

2.2.1 Optical PMD compensation techniques

Optical PMD compensators typically comprise of a polarization controlling device, an optical delay element (fixed or variable) and allied electronics which provide control signals to the optical components based on feed-back information about the link's PMD.

2.2.1.1 Classification based on PMD monitoring techniques

PMD is a randomly changing entity. Adaptive techniques are necessary to continually track the changing DGD and PSPs and perform effective PMD compensation. It is also necessary to provide reliable estimates of the DGD and PSPs to the PMD compensator. The control signals to the variable delay element and the polarization controller can be generated using different PMD monitoring techniques. A summary of the monitoring techniques used in feed-back based, optical PMD compensation systems is given below.

One of the earliest techniques used for monitoring PMD is the observation of the power levels of specific tones in the received RF spectrum of the base-band signal [8]. The monitor signal, based on which a control signal to the polarization controller is generated, is proportional to the expression:

$$1-\gamma(1-\gamma)(2\pi f_c)^2\Delta\tau^2 \qquad (2.1)$$

where, γ is the ratio of power-splitting between the two input PSPs, f_c is the center frequency of the band-pass filter for extracting the monitor signal and $\Delta\tau$ is the net DGD, from the start of the link up to and including the delay element used in the compensator [8]. The principle behind this technique is the following. PMD causes reduction of power in the main lobe of the received baseband spectrum. Therefore, the amount of PMD to be compensated for can be estimated by measuring the power level of the received baseband spectrum. The power level of a single tone (corresponding to half the bit-rate), that can give an unambiguous estimate of PMD, has been used as the monitor signal in [8]. The bandpass filter is used to extract the monitor signal from the baseband spectrum. The adjustments to the compensator are made with the goal of maximizing the monitor signal, which would happen when PMD effects are effectively nullified.

One drawback of using the above described technique is that the required hardware is bit-rate dependent. The photo-detector, band-pass filter, RF amplifiers etc can be used for one data rate only.

Another recently developed PMD monitoring technique is based on the degree of polarization (DOP) of the received optical signal. PMD can depolarize the optical signal. This in turn reduces the DOP (since DOP is a measure of the amount of optical power that is in the polarized state). The reasons for

reduction in DOP due to PMD effects in digital communication systems have been identified and described in [9] and [10].

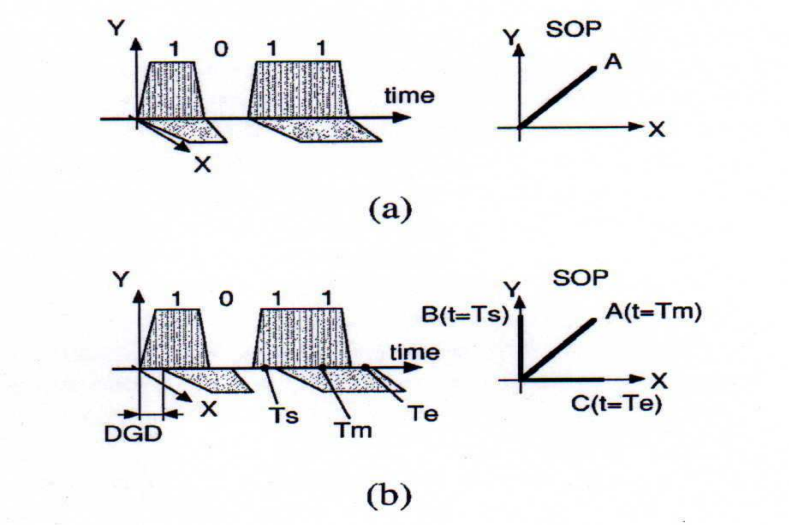

Figure 2.1 Depolarization in digital optical signals due to PMD. Comparison of cases (a) without PMD and (b) with PMD (X and Y axes correspond to the two PSPs of the transmission medium; T_s, T_m , and T_e are three different time instants at which the PMD effects on the signal are studied) [10]

Figure 2.1 illustrates the role of PMD in causing depolarization in digital optical signals. The merits of using DOP evaluation in the PMD monitoring mechanism are several in number. DOP is bit-rate independent and largely modulation format independent. To a good extent, techniques based on DOP evaluation reduce hardware complexity. On the other hand, since DOP is also affected by amplified spontaneous emission (ASE) noise and non-linear effects, it's sensitivity to PMD may get reduced in long distance fiber-optic links.

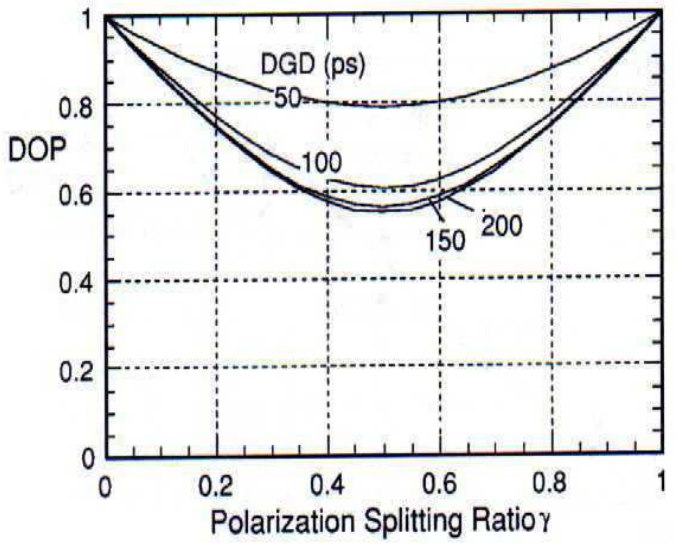

Figure 2.2 Simulated DOP versus γ, the power splitting ratio between the two input PSPs of a PMD device, for a 10-Gb/s, lithium niobate-Mach-Zehnder, NRZ (non-return to zero) modulation, for different DGD values [10]

Figure 2.2 is a plot showing the sensitivity of DOP to DGD [10]. It is significant for more than one reason. Firstly, it confirms that DOP can be a good indicator of PMD. Also, it shows that the sensitivity of DOP to DGD is greatest when the power splitting ratio, γ, is 0.5.

Another monitoring technique is based on inter-symbol interference caused by PMD in digital fiber optic systems. The received eye diagram is monitored and a control signal based on the amount of eye opening is generated. For example, the technique described in [11] uses an integrated SiGe circuit, consisting of two decision circuits, as the eye monitor. The correlation

between the bit error rate (BER) and the signal generated by the eye monitor has been reported to be good. The goal of PMD compensation in digital systems is the minimization of BER. However, the BER by itself cannot be directly used as a quantity representative of PMD, because it cannot be measured with high accuracy in a short period of time. Methods such as the eye monitor technique help to overcome such difficulties by providing a control signal which is correlated to the BER.

2.2.1.2 Classification based on order of compensation

Depending on the versatility and compensation capability, PMD compensators can be classified as half-order, first-order and second-order compensators. A half-order compensator comprises of a polarization controller and a fixed optical delay element. In addition, there is a feed-back control mechanism to provide appropriate control signals to the polarization controller. The principle of operation is that the polarization controller is adjusted so as to minimize the combined DGD of the link and the compensator. The delay element is fixed. Since this compensator can only compensate for a fixed amount of DGD, rather than varying delays, it is sometimes referred to as a half-order compensator. A half-order compensator configuration, consisting of a polarization controller and a segment of high-birefringence fiber (fixed delay element) has been described in [8]. The polarization controller adjustment was made based on a feed-back signal

which was the power level of the tone corresponding to half the data rate in the received base-band spectrum.

Figure 2.3 is a reproduction of the PMD compensator configuration described in [8].

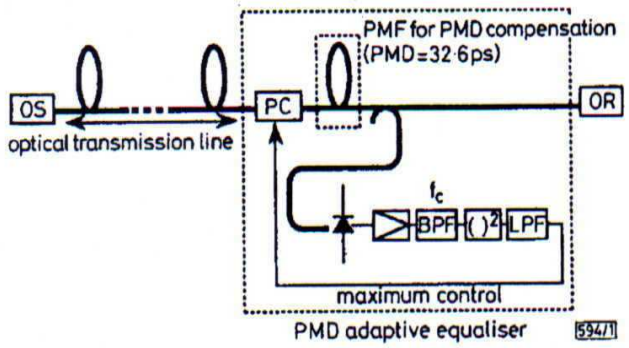

Figure 2.3 Half-order PMD compensator. (OS-optical source, PC-polarization controller, LPF and BPF-low-pass and band-pass filters, $(\ )^2$ – square-law detector, OR-optical receiver) [8]

A first-order PMD compensator is slightly more complex than a half-order compensator since it has a variable delay element instead of a fixed delay element. A feedback mechanism provides control signals for adjusting both the polarization controller and the delay element. The first-order compensator can be employed to counter different amounts of DGD values. The first-order configuration described in [3] uses a polarization controller and a variable delay element. Based on the feedback signal (which is similar to the one adopted in [8]), polarization and delay adjustments are executed so as to minimize the PMD effects. In order to increase the accuracy of the PMD

compensation, the SOP of the optical signal may be scrambled before the signal is launched into the fiber link. Figure 2.4 is a block diagram of the PMD compensation system described in [3].

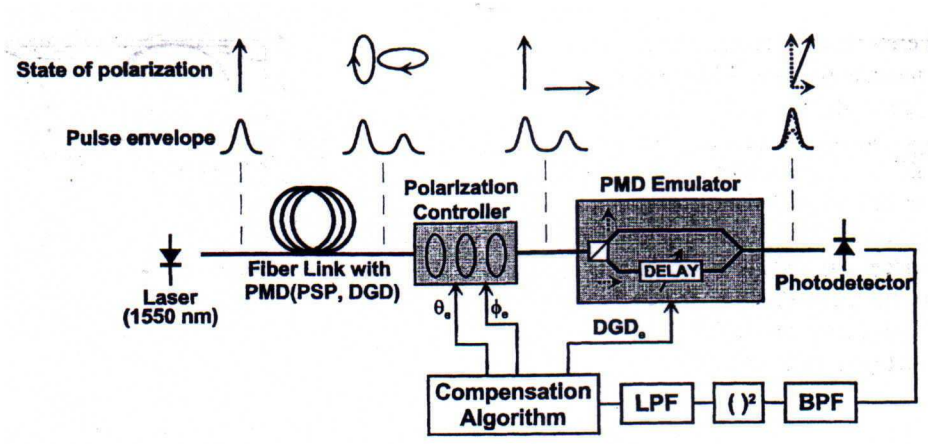

Figure 2.4 First-order adaptive PMD compensator functional block diagram. (LPF and BPF-low-pass and band-pass Filters, $(\ )^2$ - square-law Detector) [3]

A similar first-order compensator configuration is described in [12]. The polarization controller is a lithium-niobate based device. The control signals for the variable delay and the polarization controller are based on the power level of the received base-band spectrum.

A first-order compensator, using the DOP of the received signal as the feedback parameter, has been shown to compensate for PMD at data rates of 40 Gb/s and 80 Gb/s [13]. An advantage of using the DOP as the feedback parameter is that compensation can be made bit-rate independent.

Figure 2.5-b is a block diagram of a DOP feed-back based, first-order PMD compensator [14] (also referred to as a post-compensation method owing to the compensator's location on the receiver side).

Another approach for first-order PMD compensation is called the PSP transmission method. It was first described in [15]. The PSP transmission method is a pre-compensation method in which a polarization controller is used to align the SOP of the optical signal with a PSP of the fiber link. Figure 2.5-a [14] shows the block diagram of a first-order PMD compensator based on the PSP transmission method.

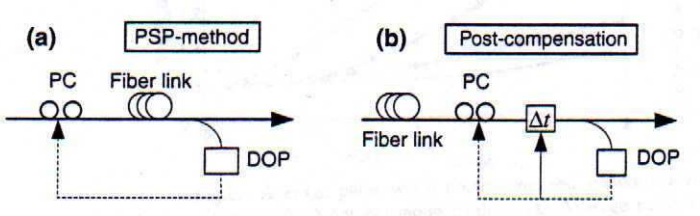

Figure 2.5 First-order PMD compensation: a) PSP method b) post-compensation method (PC-polarization controller, Δt-variable delay element) [14]

Given the increasing data-rates and the expanding bandwidth, importance has been attached to second-order PMD compensation also. One proposed configuration uses two polarization controllers and two pieces of high-birefringence fiber [16]. The compensator's PSPs are made to vary linearly with frequency so as to compensate for PMD over a larger bandwidth. The principle of changing the PSPs of the compensator as a linear function of frequency is made use of in the configuration described in [17] also. However,

the set-up adopted in [17] includes three polarization controllers and two variable delay lines (or one variable delay line and one Faraday rotator). Figure 2.6 is a block diagram of the compensator described in [16].

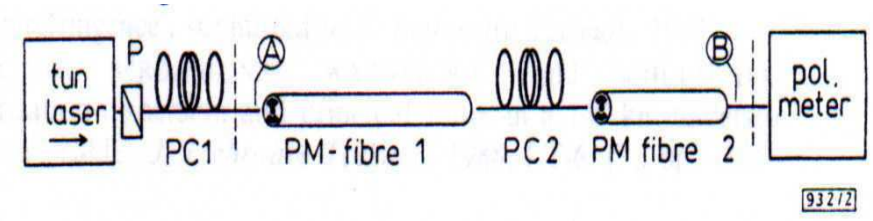

Figure 2.6 Second-order PMD compensator block diagram. (PC1 and PC2-polarization controllers) [16]

2.2.2 Electronic equalization techniques

Electronic equalization using digital filters is an attractive method for reducing inter-symbol interference (ISI). When applied to digital fiber-optic communication systems, such methods can be adopted after the receiver, to reduce ISI due to impairments such as PMD. Since they are used in the post-detection stages, the phase of the optical signals will not be available. Such electronic PMD equalizers can be integrated into the receiver, thus saving installation costs. The goal of electronic equalizers is minimization of ISI at the receiving end (regardless of the phenomenon that is causing it, be it PMD or chromatic dispersion or any other).

Some of the electronic filters used for ISI reduction are the transversal filter (TF), decision feedback equalizer (DFE) and the maximum likelihood sequence detection scheme (MLD).

The TF divides the signal into two copies, delays the copies by constant delay stages, ΔT, and superimposes the differentially delayed signals at the output port. The tap weights (C_0, C_1 etc) are adjusted to minimize ISI in the received signal [5].

The DFE is a non-linear filter. Non-linear filters are advantageous in the sense that they can improve signal quality even if the received eye-diagram is poor (severe ISI condition), unlike TF, which requires an "open" eye-diagram [5]. However, DFE requires high-speed signal processors.

The MLD scheme is based on the correlation between an undistorted signal sequence and an estimate of the received signal sequence, over many bits. The selection of the sequence and the maximization of the correlation are the factors based on which the decision for each individual bit is made [5].

A theoretical study comparing the performance of the above three schemes yielded the following result [18]. A concatenation of the TF and DFE would yield better performance than either the TF or the DFE. However, the MLD scheme provided the best possible performance.

Figures 2.7-a, 2.7-b and 2.8 illustrate the TF, DFE and MLD concepts. ΔT represents constant delay, C_0, C_1 etc. and B correspond to tap weights, V_{th} is the threshold voltage, C is the clock phase and ADC is an analog-to-digital converter [5,18].

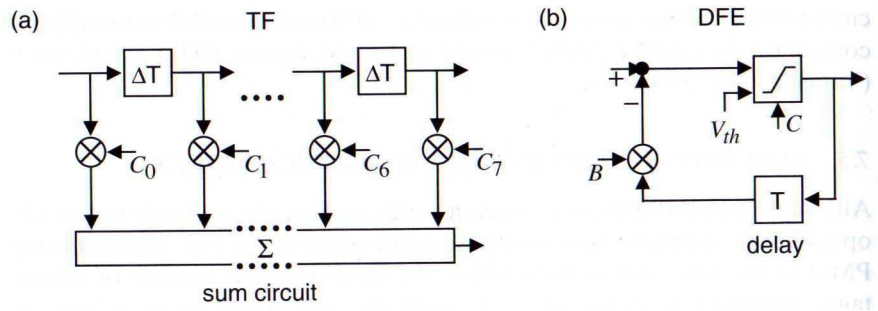

Figure 2.7 (a) The transversal filter (TF) concept and (b) the decision feedback equalizer (DFE) concept [5]

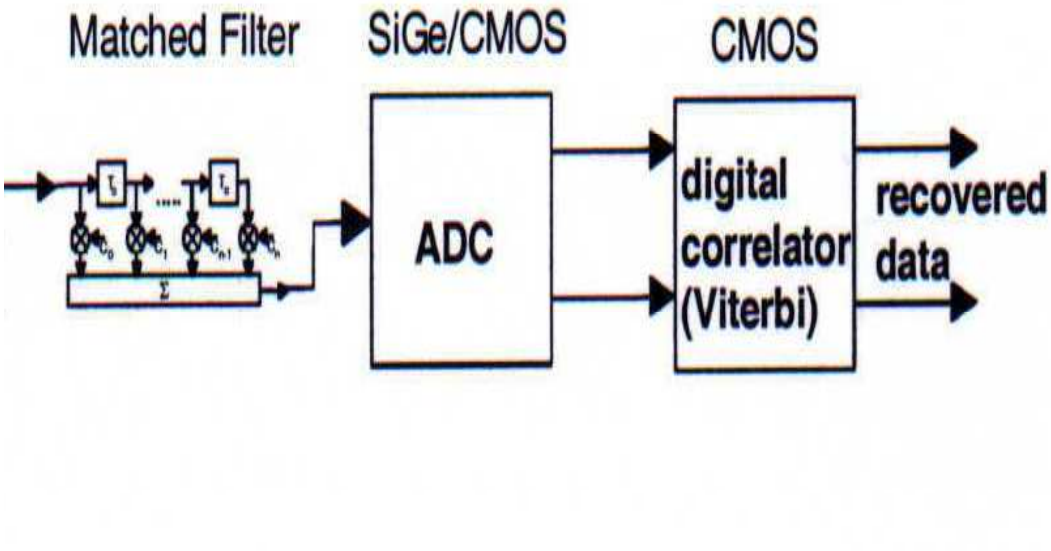

Figure 2.8 The maximum likelihood sequence detection (MLD) concept [18]

Although electronic equalization appears to be an attractive method for PMD mitigation, it has limitations. As data rates rise beyond 10 Gb/s, it will be a challenging task to perform electronic equalization because of the difficulty in finding electronic delay stages and filters that can operate at such high speeds.

2.2.3 Comparison of feed-forward and feed-back techniques for PMD compensation

So far, several examples of the feed-back method for adaptive PMD compensation were described. However, there also exists the feed-forward method of PMD compensation. Figure 2.9 shows the feed-forward and feed-back techniques.

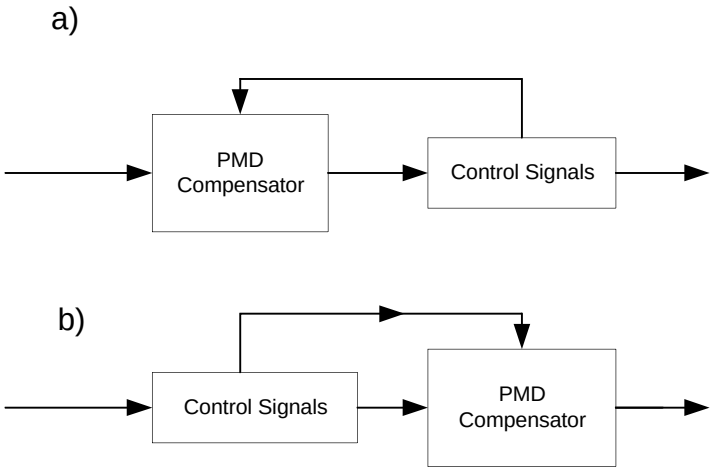

Figure 2.9 (a) Feed-back method (b) feed-forward method

A feed-forward technique, using a fixed delay element, has also been demonstrated recently [19]. The adjustments to the polarization controller are made based on real time PSP characterization using measurements from a polarimeter. A scrambler is used to rapidly change the SOP of the transmitted optical signal in order to hasten the collection of a large number of distinct polarimetric measurements. Figure 2.10 is a block diagram representation of this technique.

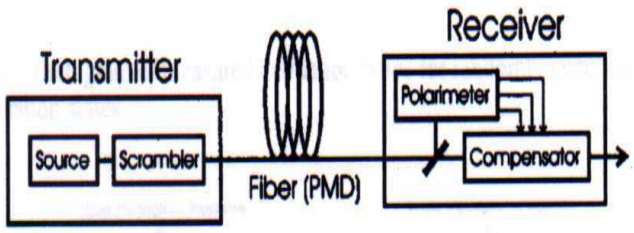

Figure 2.10 Block diagram of the proposed feed-forward PMD compensator [**19**]

2.3 Increasing PMD tolerance in a fiber-optic system

In addition to compensating for PMD, there are methods by which a fiber-optic communication system's tolerance to PMD can be enhanced. A well-researched such method is the use of PMD resistant modulation formats. Forward-error correction (FEC) coding is another example. FEC can help increase the tolerance of a system to effects of noise, chromatic dispersion and PMD. An experiment described in [20] uses Reed-Solomon error-correcting codes along with a first-order PMD compensator to effectively increase the PMD tolerance of a 10-Gb/s system.

2.3.1 Modulation formats resistant to PMD effects

The most widely adopted signaling format in contemporary fiber-optic communication systems is the NRZ (non return-to-zero). However, in recent years, novel modulation formats and their resistance to signal degrading phenomena, such as PMD, have also been studied widely.

Return-to-zero (RZ) signals are considered more resistant to penalties caused by broadening than NRZ. The reason for the increased resistance of RZ can be explained as follows [5]. In the case of RZ modulation, the signal energy is more confined to the center of each bit duration. As DGD increases, the power in isolated zeros rises only slowly. Whereas in the case of NRZ, this power rises quickly and combines with the ones to cause greater penalty [5].

In addition to RZ, there are the chirped RZ (CRZ), classical solitons and dispersion-managed solitons (DMS). which are known to be more resistant to PMD effects.

Classical solitons and DMS are considered more resistant to birefringence induced break-up. Just as dispersion and non-linearity balance each other to prevent pulse broadening, the non-linear attraction between the two polarization components prevents the break-up of a soliton or DMS pulse due to birefringence [5].

A comparison of the penalties incurred by NRZ, RZ, CRZ and DMS signals in the presence of high PMD, in a 10-Gb/s terrestrial system, has been made using computer simulation [21]. The results showed that RZ, DMS and CRZ signals performed better than NRZ for spans of up to about 600 km. For longer spans, CRZ provided the best system performance.

Examples of other modulation formats that have been studied and that are known to be more resistant to PMD than NRZ are, the phase-shaped binary transmission format (PSBT) [22] and optical duo-binary modulation which has been reported to be more resistant to higher order PMD effects also [23].

3. ADAPTIVE PMD COMPENSATION

3.1 Introduction

This chapter will focus on the adaptive PMD compensation system developed in the lightwave communication systems laboratory at the University of Kansas.

The early version of the adaptive PMD compensator consisted of a polarization controller (HP 11896A) and a PMD emulator (JDS FITEL PE3). The PMD feedback technique was similar to the one described in [8]. The control signals for the polarization controller and the PMD emulator were generated based on the power level of the tone corresponding to half the data rate, in the received baseband spectrum (eg. 5 GHz tone was considered for 10 Gb/s data rate). An algorithm was developed in order to adaptively track the varying PSPs and DGD of a link.

Several enhancements were then made to the compensator, which included the addition of a high-speed, liquid-crystal based polarization controller in place of the HP 11896A, a variable delay line and a fixed length of polarization maintaining fiber, instead of the PMD emulator, and a micro-controller to control these two devices. However, the feedback technique essentially remained the same as before. The overall speed and efficiency of the PMD compensator could be enhanced.

Still later, a need was felt to make the PMD compensator bit-rate independent and also to reduce the complexity of the hardware involved. Based on the recommendation in several publications, it was decided to change the feedback technique from one based on RF tones to the one using the received signal's degree of polarization (DOP).

The present version of the PMD compensator uses a DOP-based feedback technique. The high-speed, liquid-crystal, polarization controller, the variable delay line and the fixed length of polarization-maintaining fiber, and the microcontroller have been retained. An interface board, developed in the laboratory, is used to communicate the control signals from the microcontroller to the polarization controller and to the variable delay line.

A detailed description of the PMD compensation algorithm and the processes involved will be provided in the following paragraphs.

3.2 Description of the adaptive PMD compensation system

3.2.1 Block diagram of the system and the PMD compensation algorithm

The functional block diagram of the adaptive first-order PMD compensation system, in it's present version, is given in figure 3.1.

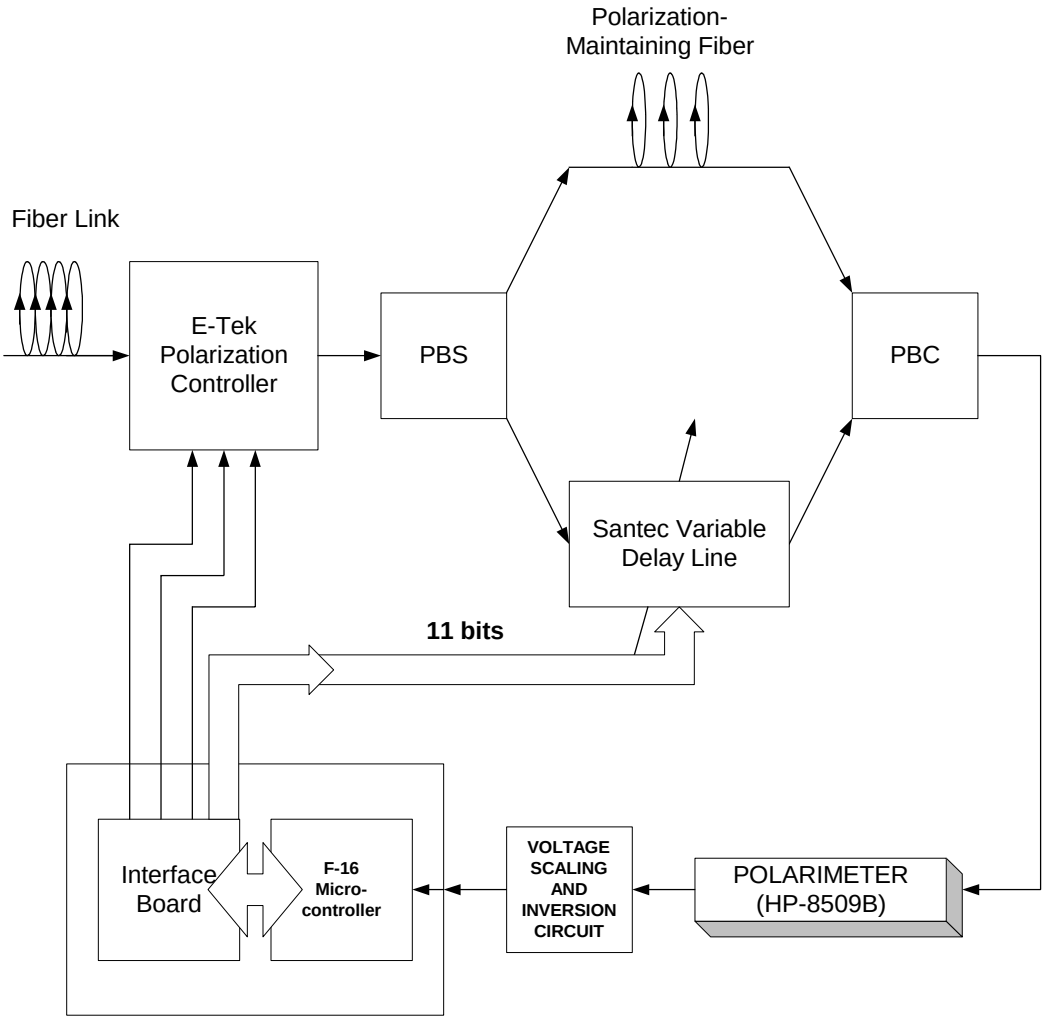

Figure 3.1 Functional block diagram of the adaptive PMD compensation system. (PBS, PBC: Polarization Beam Splitter and Polarization Beam Combiner)

The optical signal, degraded by the fiber's PMD effects, is received by the liquid-crystal polarization controller (PC). The PC is used to align the fiber's output PSPs with the input PSPs of the polarization beam splitter (PBS). (The input PSPs of the PBS are linear PSPs). This alignment is made based on the control signals sent separately to three liquid-crystal cells inside the PC.

The two paths following the PBS carry the two orthogonal components of the received optical signal that have been differentially delayed in the fiber link. The compensation algorithm performs adjustment of the PC cells so that the slower component travels along the path with the fixed length of polarization maintaining fiber (high birefringence fiber) and the faster component travels along the path that contains the variable delay line. The delay line is adjusted (based on it's control signal) so that the fast component is delayed just enough to match the slow component. The two components are combined in the polarization beam combiner (PBC). Polarization-dependent loss (PDL) in the compensator has to be kept at a minimum in order to perform accurate compensation. This can be ensured by seeing to it that the attenuation in the two paths (after the PBS) are nearly the same. Steps were taken to achieve this by carefully bending the fixed length of PMF and inducing the right amount of attenuation so that the net PDL was minimized. The PDL is currently less than 0.2 dB (for most of the positions of the delay line).

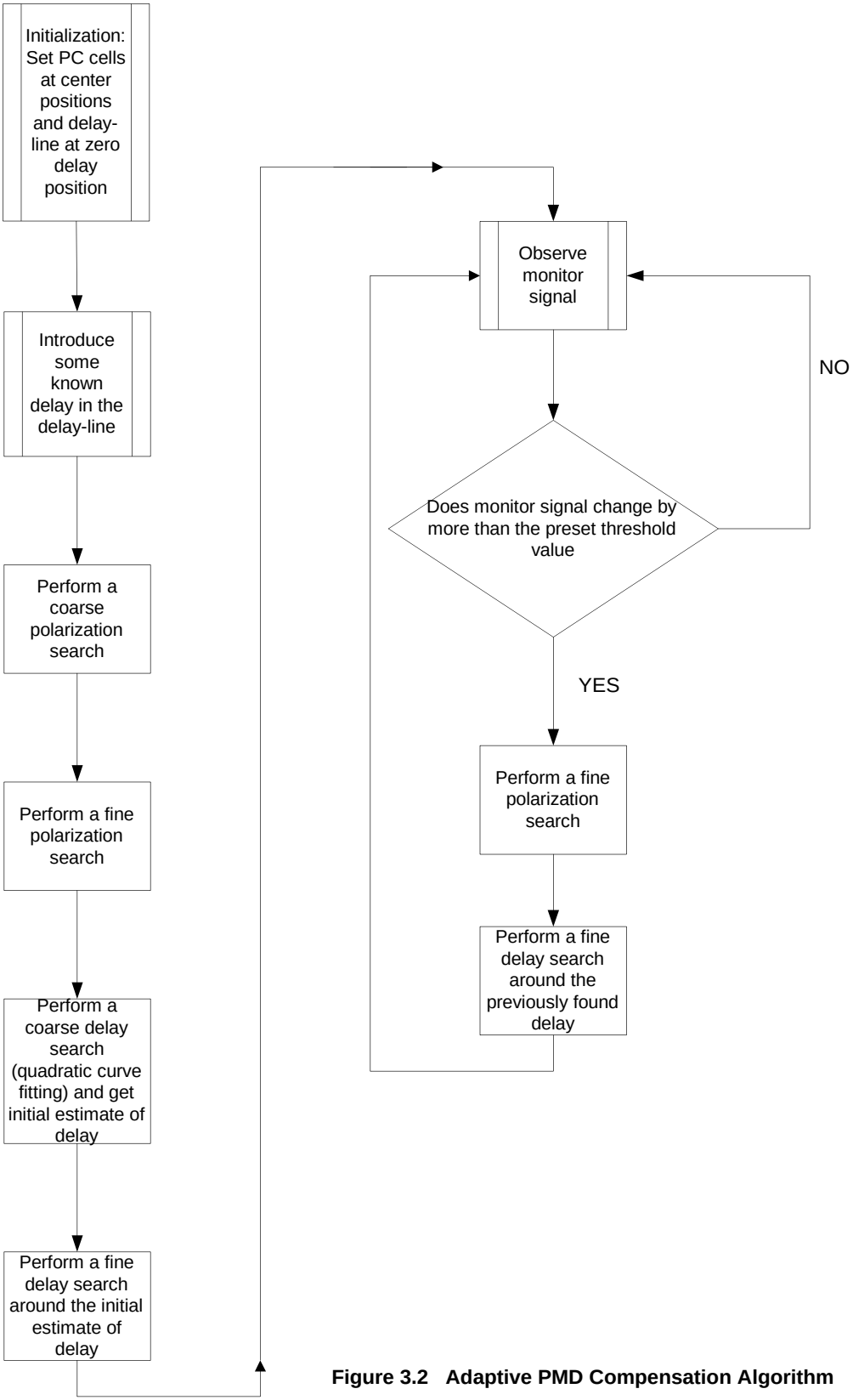

Figure 3.2 Adaptive PMD Compensation Algorithm

The steps in the PMD compensation algorithm, from the start to the end, are given in the form of a flow-chart (figure 3.2) in the previous page. The steps in the algorithm will be explained in detail in the following paragraphs.

3.2.2 Operation and control of the polarization controller

The polarization controller (E-Tek FPCR-B23157111) has four liquid-crystal cells, out of which only three are used for the PMD compensation application. In order to achieve any arbitrary output polarization state, three cells are sufficient. The polarization controller (PC) is used to align the fiber link's output PSPs with the input PSPs of the PBS (which are linear PSPs).

For performing accurate compensation of the delay between the differentially delayed components of the optical signal, it is necessary to split the components just *as* they arrive at the fiber's output PSPs. Therefore, proper alignment between the fiber's output PSPs and the input PSPs of the PBS is essential. How do we make sure that these two pairs of PSPs are properly aligned? What role does the PC play in achieving this alignment and how does it do it, are all the questions that will be answered in this section.

The basic principle of liquid-crystal based devices is that their retardance is modified depending upon an externally applied voltage. The retardance is dependent on the alignment of the "grains" in the liquid-crystal material, which actually is influenced by the external voltage. Therefore, by applying a changing voltage to a liquid-crystal cell, different alignments of the grains can

be attained, which in turn produce different orientations of orthogonal polarization axes. Three such cells in the PC can be controlled to obtain any of the polarization orientations that exist in Stokes space. The two orthogonal components of an optical signal that is input to the PC, can thus be controlled to travel along a desired set of orthogonal polarization axes (or principal states). Figure 3.3 is a diagrammatic representation of the purpose of using the PC in the PMD compensation system.

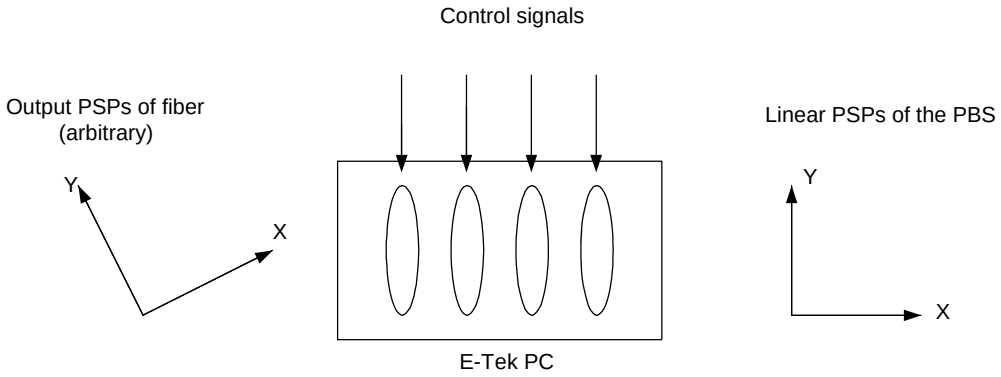

Figure 3.3 Position of the PC and it's purpose in the compensation system

The maximization of the monitor signal is the goal based on which adjustments to the PC are made. At the start of the PMD compensation process, the variable delay-line is positioned to provide a positive delay (which usually is a rough estimate of the actual amount of delay to be compensated for). Following this, the cells in the PC are adjusted one after the other with the aim of maximizing the monitor signal. It should be noted here that the magnitude of the monitor signal will be maximized when PMD is minimized. For this to happen, first, the alignment between the fiber's output

PSPs and the input PSPs of the PBS should be such that the fiber's fast output PSP is aligned with the PSP leading to the delay line (which is set at a non-zero delay value) and the fiber's slow output PSP is aligned to the PSP leading to the fixed length of high birefringence fiber.

The voltages that are applied to the three cells in the PC are generated in the interface board. Each voltage is an alternating voltage with a frequency of about 1.4 MHz, with a peak-to-peak amplitude of 6 V. The operation of the cells was found to be independent of the frequency of the alternating voltage (Appendix A). However, it is sensitive to the amplitude. The value of 6 V peak-to-peak was found to be sufficient to induce one complete rotation of the resulting polarization state, in Stokes space. The voltage can be adjusted to any value between 2 and 12 V peak-to-peak (Appendix A).

During the PMD compensation process, one cell is taken up at a time. Initially, the alternating voltage is applied in large (coarse) steps and a "coarse" search is conducted over the entire voltage range of 6 V. The voltage to a cell is fixed at that step for which the monitor signal is maximized. The voltage thus fixed will correspond to a unique polarization point in Stokes space. A similar "search" is performed on the following cell. The terminating polarization point of the previous search will act as the starting point of this new search. The rotation axis for the new search will be orthogonal to the

previous search's rotation axis In this way, a unique set of orientations using the three cells, that maximize the monitor signal, can be obtained.

In the actual implementation of the PMD compensation algorithm, the peak-peak voltage of 6 V has been broken-down into 104 equal-sized voltage steps. One coarse step-size is equivalent to 8 of the voltage steps. Or, in other words, one coarse step size corresponds to about 0.46 V. Figure 3.4 is an oscilloscope picture of the voltage that is supplied to each cell in the PC.

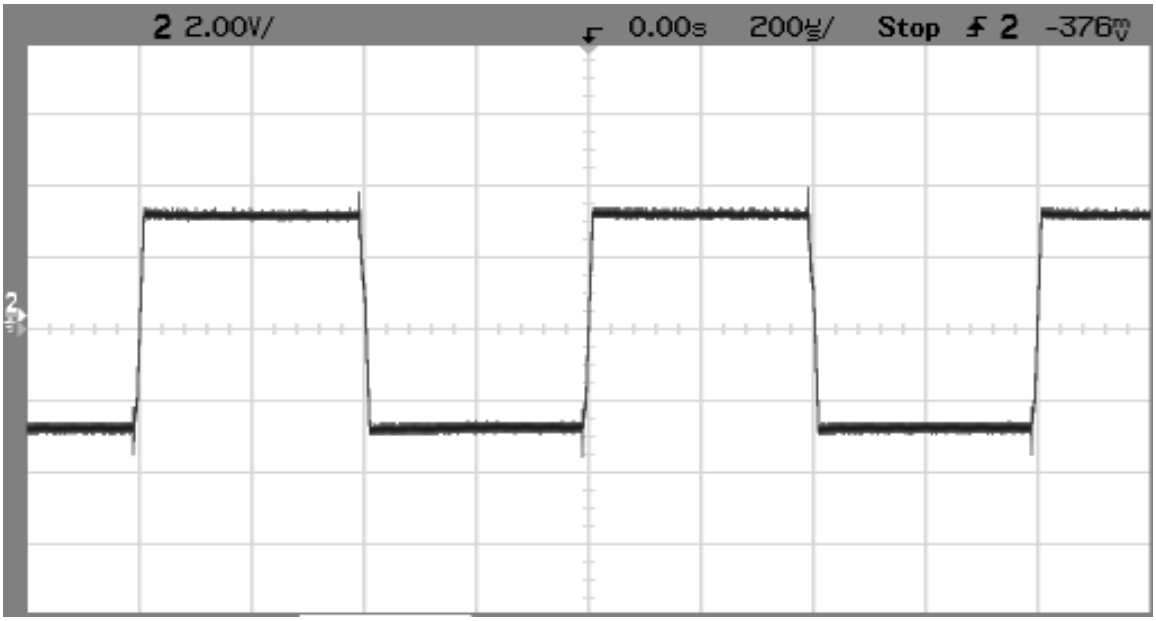

Figure 3.4 Oscilloscope picture of the control voltage supplied to a cell in the PC

After the coarse search, a fine search, which has a smaller voltage step size, is conducted using each cell. The step size for the fine polarization search is 1 voltage step or about 0.0575 V. The maximum range of the fine search is 4 steps on either direction of the starting point (which is that polarization point which resulted from the coarse search).

An interface board, built in the laboratory, is the link between the microcontroller and the PC and delay line. The interface board contains separate "channels" that generate the voltages that are provided to the liquid crystal cells. It also contains a circuit that provides a 11-bit TTL signal for controlling the delay line (see Appendix A for a detailed description of interface board).

3.2.3 Operation and control of the variable delay line

The variable delay line (Santec ODL-620) uses a stepper motor to alter the propagation distance of the light entering into it. It contains a collimator at the input, a prism (whose position is altered by the stepper motor) and a collimator at the output. The stepper motor expects to receive an 11-bit TTL digital code, which is provided by the interface board. The delay adjustments are made based on the bit combinations in the 11-bit code. The maximum range of the delays that can be set using the delay line is 300 ps and the number of steps is 1800. The resolution or the delay per step is about 0.167 ps.

During the PMD compensation process, the monitor signal varies in an approximately quadratic fashion, with variations in the delay-line setting. The maximum point of this quadratic curve is achieved when the delay setting in the delay-line is such that net PMD of the fiber link and the compensator is minimized [24].

After the coarse and fine PC searches are complete, a coarse delay search is performed in order to obtain an initial estimate of the delay. The coarse delay search is the process of recording the monitor signal values for a set of seven settings in the delay-line. A starting delay value is chosen (which usually is a rough estimate of the delay to be compensated). The delay line is positioned at three settings on either side of the starting value of delay, with a step size of 10 ps. For example, if the starting delay value is 30 ps, the delay-line is sequentially positioned at 0, 10, 20, 30, 40, 50 and 60 ps, and the monitor signal value for each of these positions is recorded. Once the monitor signal values for all the seven delay positions are recorded, a quadratic curve fitting procedure is undertaken, using which the delay corresponding to the maximum of the recorded monitor signal values is calculated.

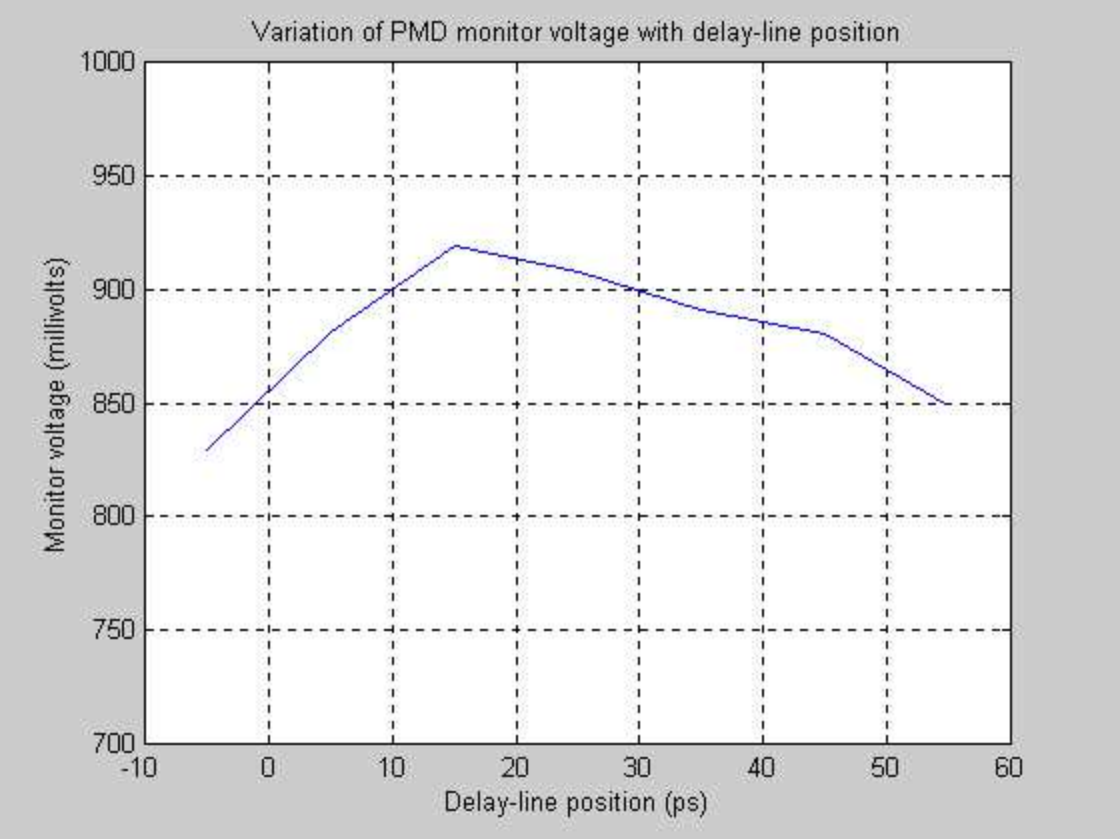

Figure 3.5 Measured variation of the PMD monitor signal with changes in delay-line position

Figure 3.5 is a plot of the measured variation of the monitor signal for different positions in the delay-line (DGD emulated in the system was 30 ps).

A fine delay search is then performed about the newly calculated delay value. The step size for the fine delay search is 1 ps and the number of steps is five on either side of the delay calculated from the coarse search.

3.2.4 PMD monitor signal and the feedback path

The early development of the PMD compensation system was based on an RF monitor signal. Figure 3.6 below shows the early implementation of the feedback path in the compensation system and the components involved [24]. The feedback path consisted of a photodetector, a microwave spectrum analyzer and a computer for controlling the PC (HP 11896A) and the PMD emulator (JDS FITEL PE3). The microwave spectrum analyzer was used to extract the 5-GHz tone from the received base-band spectrum. The computer provided control signals to the PC and the PMD emulator, based on the power level of the monitor signal.

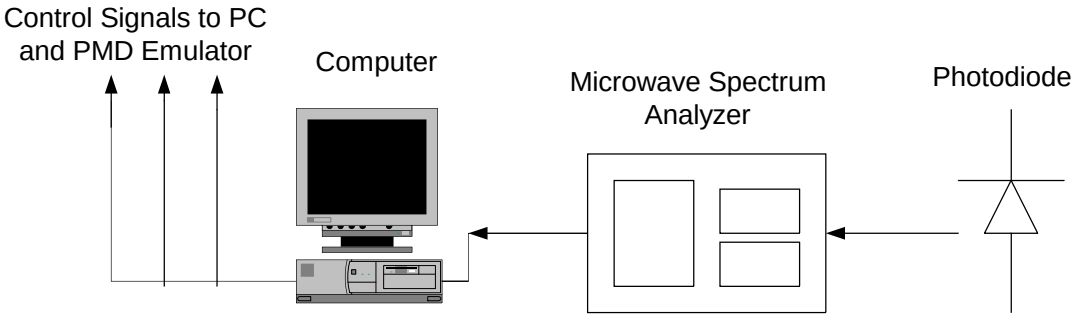

Figure 3.6 Feed-back path in the early version of the PMD compensation system [24]

Subsequently, some components in the feedback path were replaced with faster ones. The feedback technique, however, remained unchanged. Figure 3.7 shows the feedback path with additional components to extract the monitor signal.

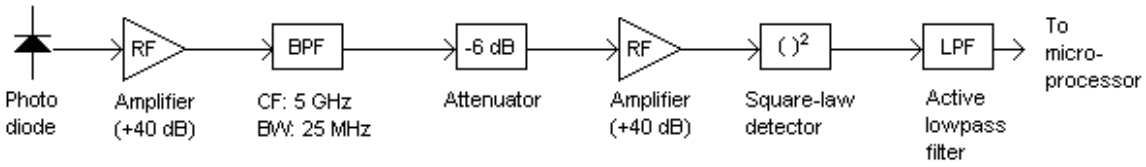

Figure 3.7 PMD compensation system feed-back circuit; BPF: bandpass filter, CF: center frequency, BW: bandwidth (designed and drawn by Juan M. Madrid)

In order to make the compensation system more compact, a band-pass filter was added to extract the monitor signal. A square-law detector, power amplifiers and a low-pass filter completed the feedback path. The voltage signal at the output of the low-pass filter was provided to an A-D port of the microcontroller, which in turn communicated with the interfaces for the PC and the delay-line for providing control signals. Subsequently, another similar path was added to extract the 1-GHz tone also, from the base-band spectrum. It was found that the power level of the 5-GHz tone was unstable (believably due to PDL). This often resulted in ambiguities during the PMD compensation searches. The power level of the 1-GHz tone was also seen to fluctuate due to PDL. However, the 1-GHz tone was found to be insensitive to changes in PMD. Therefore, it was decided to normalize the power level of the 5-GHz tone by using the power level of the 1-GHz tone in order to reduce the PDL induced instabilities of the monitor signal. The two power levels (5-GHz and 1-GHz) were provided to separate A-D channels in the micro-controller and the normalization was performed digitally through additional instructions in the PMD compensation program.

Certain issues such as stability of the monitor signal were faced with the above set-up. There was also a growing need to transform the PMD compensation system into a bit-rate independent entity. It was then decided to switch to using the degree of polarization (DOP) of the received signal as the monitor signal (rather than RF tones).

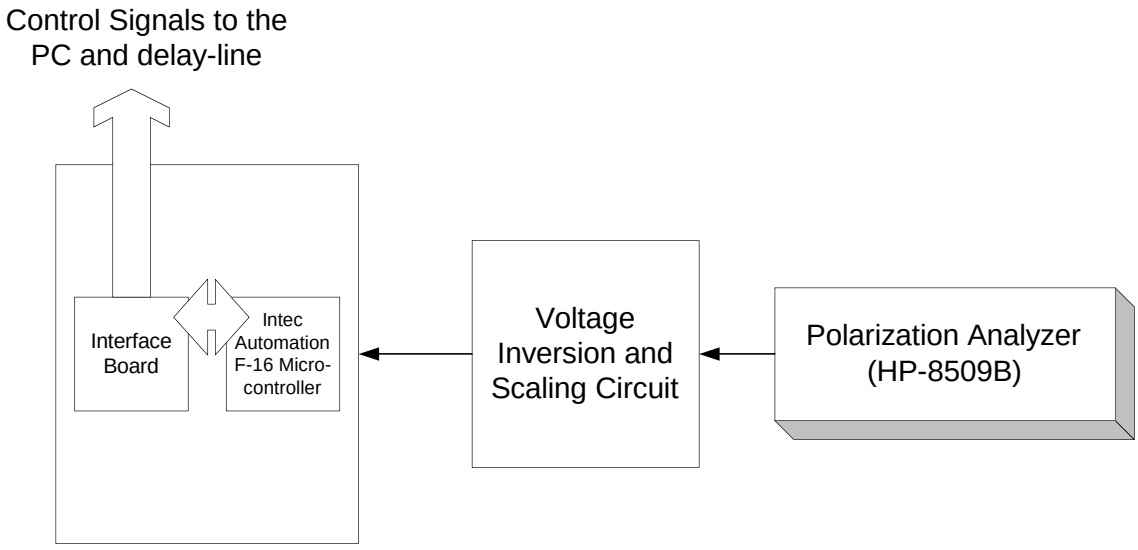

Figure 3.8 Feed-back path in the present version of the PMD compensation system

The feedback path that is currently in place is shown in figure 3.8. The feedback path consists of a polarization analyzer (HP 8509B), which is capable of continuously measuring the DOP and providing an equivalent analog voltage output. It should be mentioned here that any device that is capable of measuring and providing the DOP information can be used in the place of the HP 8509B. An example of such a device is the Inline Polarimeter™ manufactured by General Photonics Corporation, Chico, CA,

USA. However, while using different DOP measuring devices along with the PMD compensation system, due consideration must be given to the speed of measurement of the DOP (sampling rate).

A simple circuit is used to perform inversion and scaling of this analog voltage (see Appendix B for the circuit diagram) in order to make it acceptable to the microcontroller. Thus, an analog voltage between 0 and 5 V is supplied to one of the analog-to-digital (A-D) ports of the microcontroller. A computer program is used to communicate with the microcontroller and enable it to perform operations required to generate and send control signals to the PC and the variable delay line.

3.3 Polarization scrambling and it's application in adaptive PMD compensation

3.3.1 Introduction

In this section, polarization scrambling and it's application in adaptive PMD compensation will be described. First, the need for polarization scrambling in PMD compensation systems, will be discussed. Following that, the principle of operation of the lithium-niobate based, single-axis, Ramar™ polarization scrambler, that was used for some of the earlier tests on the PMD compensation system will be outlined. Next, an outline of the operation of the fiber-squeezer type polarization controller (from General Photonics™) will be provided.

3.3.2 Application of polarization scrambling in PMD compensation systems

The orientation of the output PSPs of a fiber link change with time due to physical factors such as a stress and temperature. To perform compensation of the delay between the differentially delayed components of the received optical signal, knowledge of the output PSPs of the fiber link is necessary. The estimates of the output PSPs (and DGD), based on the PMD monitor signal, will be accurate only when the signal power is equally distributed between the fiber's PSPs [3]. However, this condition is not always guaranteed. The SOP of the optical signal also varies with time and therefore, over time, the power distribution between the PSPs ranges between a minimum and maximum. The minimum corresponds to the scenario when the SOP is aligned with one PSP (so that all the optical power is aligned to one PSP) and the maximum corresponds to the scenario when the optical power distribution among the PSPs is equal. To understand better the significance of the power distribution between PSPs, let us consider equation (1.3). The PMD induced penalty ε, is dependent on the value of γ, the power splitting ratio between the two PSPs. Therefore, to assess the true extent of PMD, the worst case effect has to be considered. And this is the case when the power distribution between the PSPs is equal (i.e., γ=0.5).

When the SOP is scrambled (randomly changed), at a rate higher than the PMD compensator's sampling rate, each sample of the PMD monitor signal

represents a different SOP. Therefore, when many such samples are taken and their average is used, the effect is similar to the case when γ=0.5 (i.e., the PMD compensator actually takes into account the worst case PMD effect). The significance and application of polarization scrambling in PMD compensation systems was first studied and demonstrated in [3]. In practical scenarios, the polarization scrambling may be performed after the signal emerges from the intensity modulator.

3.3.3 Polarization scrambling and the adaptive PMD compensation system

The polarization scrambler that was initially used along with the PMD compensation system was a lithium-niobate based, single-axis polarization scrambler from Ramar™ corporation. It is essentially a phase modulator, but with a 45° polarization rotator in-built into it's input port. The 45° rotation causes the input optical power to get distributed along both the principal axes. When an external, alternating voltage is applied, the phase of the electric field component along the horizontal principal axis changes (while the vertical component remains unchanged) and thus the resulting output polarization states change. The changes in the resulting polarization states are confined to one axis in Stokes space and so, it is referred to as a single-axis polarization scrambler. Or in other words, the SOP changes map out a great circle on the Poincare sphere, which is a graphical representation of Stokes space (see section 3.3.4 for detailed definition of Poincare sphere).

Later, a fiber-squeezer type device from General Photonics™ corporation (Polarite II) was used with the PMD compensation system. The device is a four-axis polarization controller, which can be used for polarization scrambling also. It has four piezo-electric actuators that squeeze a small length of fiber from different directions. Therefore, when two or more axes are operated, the resulting SOP changes are spread all over Stokes space or in other words a full coverage on the Poincare sphere is obtained. An electronic amplifier amplifies the input voltage signals and provides the necessary voltages to the piezo-electric actuators.

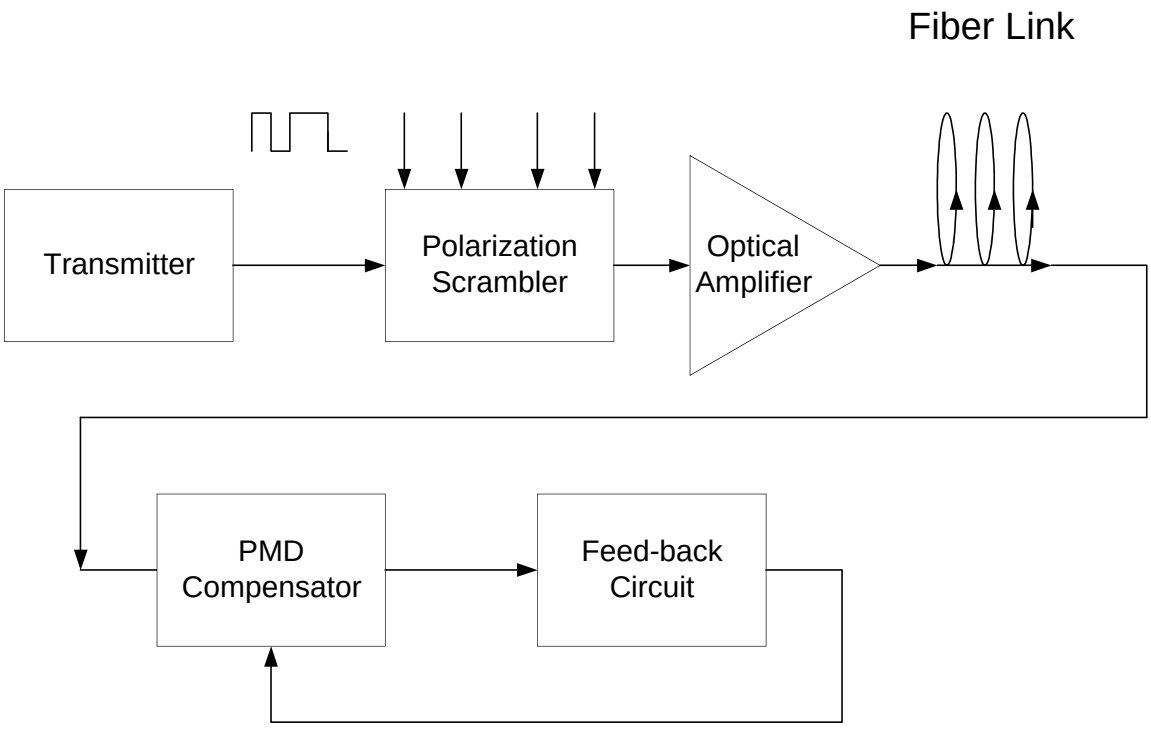

Figure 3.9 Position of the polarization scrambler in a PMD compensation application

Figure 3.9 shows the typical position of a polarization scrambler in a PMD compensation application.

3.3.4 Polarization concepts and DOP measurement in the HP-8509B

All the experiments performed on the PMD compensation system and reported in this thesis document involved the HP 8509B. Therefore, it will be useful to describe here the method of DOP measurement that is being followed inside it.

The phrase Stokes space has been used several times so far in this report. Stokes space and Stokes vector are entities that are used to describe the state of polarization (SOP) of an optical signal. The Stokes vector is a set of four optical power values, called Stokes parameters, that are defined in order to uniquely describe the SOP of an optical signal (see [25] for the complete definition of the Stokes parameters). The Stokes parameters are denoted as S_0, S_1, S_2 and S_3. S_0 is the total optical power. S_1, S_2 and S_3 are the optical power values in certain reference polarization states. In most practical applications, the latter three parameters in the Stokes vector are normalized using the first parameter to yield three values that range between -1 and 1. These values are called the normalized Stokes parameters which are denoted as s_1, s_2 and s_3.

The Poincare sphere is a graphical display tool in real, three-dimensional space that is used for diagrammatically representing Stokes space. It is most useful for displaying the SOP data on a screen. Any SOP can be uniquely represented on or within this unit sphere (using the three normalized Stokes parameters), which is centered on a rectangular *xyz* system [25]. Circular

states of polarization are located on the sphere's poles, linear polarization states appear on the equator and elliptical states occupy points between the equator and the poles. Completely polarized signals (DOP being one hundred percent) will be located on the surface of the sphere, while partially polarized signals will be located within the sphere. A fully depolarized signal (DOP being zero percent) will be located at the sphere's center.

The DOP, which is a measure of the fraction of optical power that is in the polarized state, can be represented as follows [25]:

$$\text{DOP} = \frac{P_{polarized}}{P_{polarized} + P_{unpolarized}} \tag{3.1}$$

where, $P_{polarized}$ and $P_{unpolarized}$ are the optical power values in the polarized state and in the un-polarized state respectively.

DOP is related to Stokes parameters and the normalized Stokes parameters through the relations [25]:

$$\text{DOP} = \frac{\sqrt{S_1^2 + S_2^2 + S_3^2}}{S_0} \tag{3.2}$$

$$\text{DOP} = (s_1^{\,2} + s_2^{\,2} + s_3^{\,2})^{\frac{1}{2}} \tag{3.3}$$

where, S_1, S_2, S_3 are the Stokes parameters and s_1, s_2 and s_3 are the normalized Stokes parameters. S_0 is the total optical power.

The HP 8509B measures the Stokes parameters and uses signal processing techniques to calculate the DOP. There is a time-constant associated with the DOP measurement process. The measurement sampling frequency was found to be nearly 2500 Hz (see section 4.2). The instrument provides a user-definable feature called *display update rate*, which is the number of samples that are taken before calculating the DOP. For all the PMD compensation applications described in this thesis report, the display update rate was set at 1000 (which is the maximum) in order to maximize the DOP measurement accuracy. Measurement averaging, which can also be user-defined, was turned-off for the PMD compensation application, in order to always obtain the instantaneous DOP values.

4. EXPERIMENTS AND FINDINGS

4.1 Introduction

This chapter will describe the tests conducted to evaluate the performance of the adaptive PMD compensation system. It will contain the description of the set-up used for the field trial of the PMD compensation system and will provide details about some experiments relating to polarization scrambling axes and frequencies.

4.2 Operating speed of the PMD compensation system

One of the first performance tests to be conducted on the PMD compensation system was the test of operating speed. At present, the PMD compensation takes nearly 100 s to complete one full cycle of searches. The initialization process requires 6 s and the coarse and the fine polarization searches together require 7 s. The coarse delay search requires about 27 s while the fine delay search requires about 58 s. A tracking cycle (which consists of one fine polarization search and one fine delay search) requires 48 s.

4.3 Experiment to fix the range of acceptable scrambling frequencies

A set of experiments was performed to fix a suitable range of scrambling frequencies to be adopted for the PMD compensation system. The experiments were performed using the lithium-niobate based Ramar™ 100 MHz, single-axis polarization scrambler. Later experiments used a fiber-

squeezer type polarization controller, from General Photonics™, which was used to perform endless polarization rotation (polarization scrambling).

The upper limit of scrambling frequency is influenced by the sampling rate of the DOP (degree of polarization) measurement device (which in this case is the HP-8509B polarization analyzer). To obtain a reliable measure of it's DOP, the state of polarization (SOP) of an optical signal must be fairly stable during the measurement sampling interval. For this purpose, polarization scrambling has to be carried out at a frequency significantly lower than the DOP measurement sampling frequency.

To determine the sampling rate of the HP-8509B, the analog voltage equivalent of the DOP was observed in an oscilloscope. Polarization scrambling was performed to intentionally change the DOP, in order to view the sampling rate information on the oscilloscope. This method revealed the sampling frequency, which is nearly 2500 Hz.

Figure 4.1-a and 4.1-b on the following page show the experimental set-up and the oscilloscope display of the DOP analog voltage when the input optical signal was scrambled at 1000 Hz. The display update rate, which is the number of samples that is taken before a DOP calculation is made, was set at 400. Measurement averaging was switched on and the number of

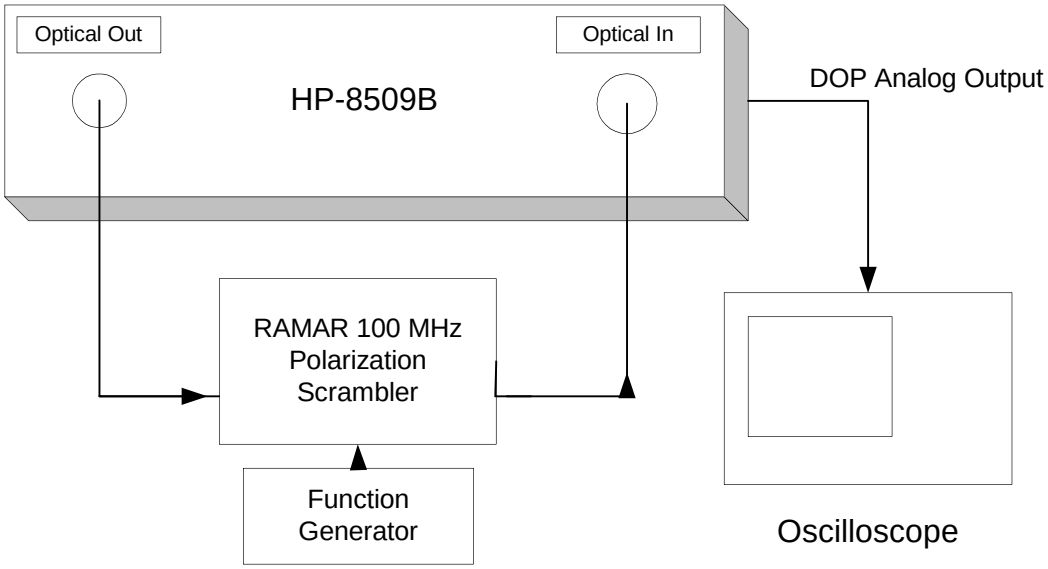

Figure 4.1a Experimental set-up for finding the DOP measurement sampling frequency

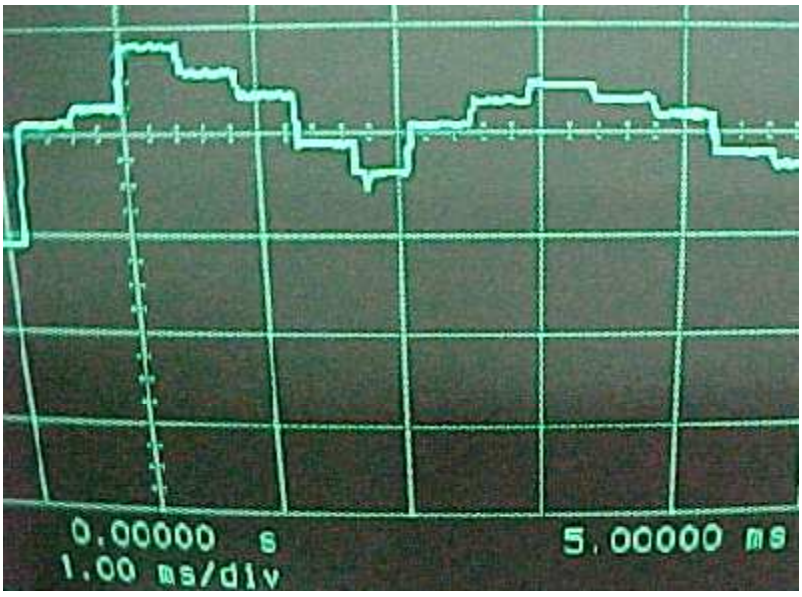

Figure 4.1b Oscilloscope picture obtained for finding the DOP measurement sampling frequency

points (instantaneous DOP values) taken for finding each average was set at 15.

To ensure SOP scrambling produced minimal interference on the DOP measurement, a polarization scrambling frequency less than a few hundred hertz was selected.

The lower limit of the scrambling frequency is influenced by the sampling frequency of the PMD compensation system. The PMD compensation algorithm performs sampling of the monitor signal using one of the A-D channels available in the micro-controller. A number of samples is taken and their average is found. Each time the algorithm seeks a monitor signal value for operating the polarization controller or the delay-line, such an average is used, rather than a single sample. The averaging is very important, for it ensures that the algorithm will take into account many different samples that represent different SOP orientations before the fiber link. In this way, the effect of scrambling the SOP, before the optical signal is transmitted into the fiber, is seen by the compensation algorithm.

It was found that the A-D sampling frequency in the micro-controller (which uses a Motorola 68HC16 micro-processor) was nearly 4200 Hz. The number of samples that are taken and averaged before a single monitor signal value is provided to the compensation algorithm has been fixed at 84 samples. This

fixes the sampling frequency of the PMD compensation system at 50 Hz. Therefore, 50 Hz will be the lower limit of the polarization scrambling frequency. A scrambling frequency less than 50 Hz could lead to incorrect PMD compensation decisions. Based on the above findings, it was decided to restrict the frequency of scrambling to between 50 Hz and 200 Hz.

4.4 Optical signal to noise ratio (OSNR) tests on the PMD compensation system

4.4.1 Description of experimental set-up and measurement method

To assess the performance of the PMD compensation system, several tests were conducted. An important test that will provide information about the robustness of the PMD compensation system while being used in multi-span, amplified, lightwave communication systems is the optical signal to noise ratio (OSNR) test. The intention was to determine the minimum received OSNR at which the PMD compensator can compensate for PMD satisfactorily.

Figure 4.2 is the experimental set-up that was used to perform the OSNR test.

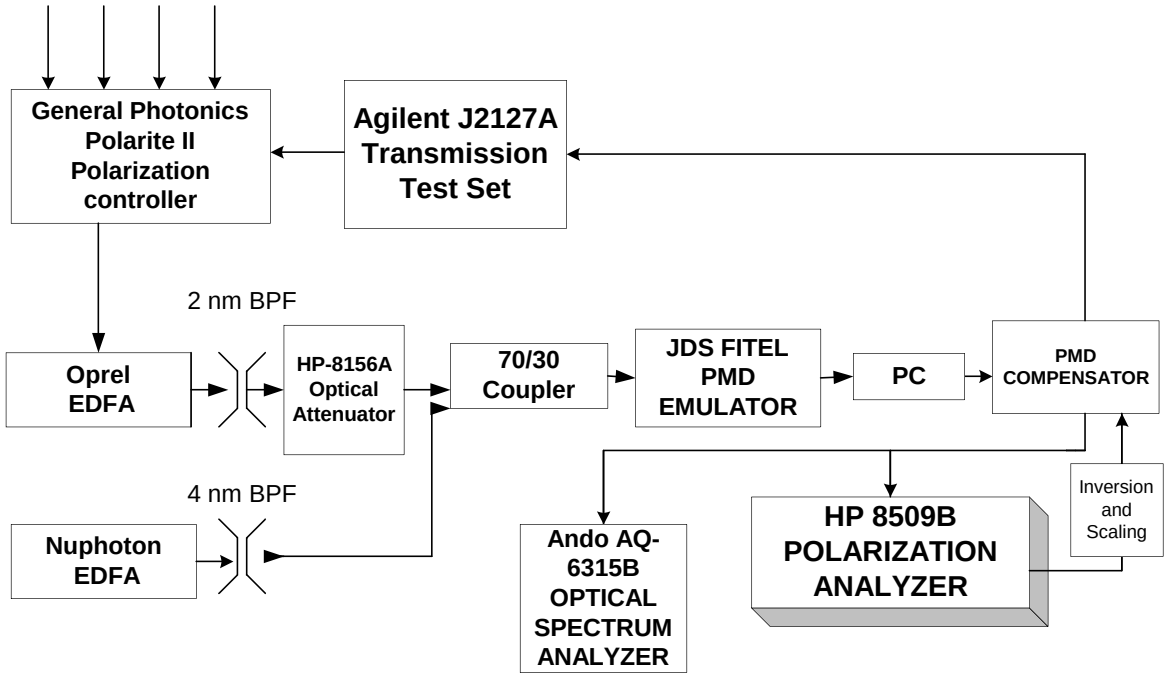

Figure 4.2 Experimental set-up for performing OSNR tests on the PMD compensation system (PC-paddle-type polarization controller; BPF- optical band-pass filter)

The Agilent™ J2127A transmission test set was programmed (menu-driven) to provide an OC-192 signal. The wavelength emitted by the test set, at this date rate, is 1534 nm. The test set is capable of measuring the bit-error rate (BER). Next, the General Photonics™ polarization controller was used to perform polarization scrambling. Three function generators were used to provide four alternating waveforms for performing four axes scrambling. The frequencies adopted were between 50 Hz and 80 Hz. Two pairs of EDFAs and bandpass filters (BPF) were used in the set-up. The Oprel™ EDFA was used

for amplifying the transmitted signal. The variable optical attenuator (HP-8156A) was used for varying the signal power. The NuPhoton™ EDFA, served as an amplified spontaneous emission (ASE) noise source. The amplified signal and the added noise were summed using a coupler. The use of a separate noise source simplified the process of varying the received OSNR.

The PMD emulator was used to set different levels of differential group delay (DGD). A polarization controller (paddle-type) was included after the PMD emulator in order to provide a means for adjusting the output PSPs of the PMD emulator.

Provision was made for monitoring the signal at the output of the PMD compensator in an optical spectrum analyzer (OSA, Ando™ AQ 6315B). The functions in the OSA were employed for measuring the OSNR. The HP-8509B was used for performing DOP measurement and providing the PMD monitor signal to the compensator, via the voltage inversion and scaling circuit.

The following method was used to measure the received OSNR. To measure the signal and noise powers, the *Search L1-L2* and *Analysis-Power* soft keys, available in the OSA, were used. The Search L1-L2 key, when enabled, takes into the account all the power between the two line markers L1 and L2. The

line markers can be positioned in any desired location using the *Marker* key. The *Analysis-Power* key measures and displays the power that is accounted for by the *Search L1-L2*.

While measuring the signal power, the line markers L1 and L2 were positioned on either side of the signal peak. When the *Analysis-Power* soft key was pressed, the power between the two line markers L1 and L2 was measured and displayed (since the *Search L1-L2* key had been activated). It has to be mentioned here that in this way, the noise power that exists between the two line markers is also included in the signal power calculation. However, the noise power thus included was found to be very small and thus could be neglected without causing any significant amount of error in the final OSNR calculation.

For obtaining the noise power a slightly different approach was adopted. The line markers were positioned such that the total power (signal + noise) could be measured. Then, from this quantity, the signal power was subtracted, to yield the noise power.

Using the signal and noise power values, the OSNR was readily calculated. The description of the soft keys and functions that were used for the power measurement have been provided in the Ando 6315B user manual (pp 5-27 and 5-45). For all the measurements, the resolution band-width in the optical

spectrum analyzer was set at 1 nm. The wavelength span was set from 1530 nm to 1540 nm. The power reference level was -5 dBm and the Y-axis scale was 10 dB/division. It was observed that while using the *Search L1-L2* and *Analysis-Power* keys, the measured power was largely independent of the resolution bandwidth and the wavelength span settings.

All the BER measurements were made at the point where the signal entered the HP 8509B (receiver). Each BER measurement was carried out for a duration of about 10 minutes. After fixing an OSNR of 10 dB, the BER with 0 ps emulated DGD and with the compensator set at it's initial condition (when the polarization controller cells are in their center positions and the delay-line is set at the zero delay position) was measured. Following this, the BER with 10 ps emulated differential group delay (DGD), with the compensator still in it's initial condition, was measured. Then, the compensator was allowed to run a compensation cycle. Once a satisfactory result was obtained, the BER was again measured. In this way, the BER before and after compensation could be determined. Similarly, BER measurements were made with emulated DGDs of 20, 30 and 40 ps. This process was repeated for OSNR values of 8, 6 and 4 dB. For the OSNR of 10 dB, one additional set of measurements with emulated DGD of 50 ps was recorded. The results are given below.

4.4.2 Results obtained

Table 4.1 Measured BER for 0 ps emulated DGD with the compensator in it's initial condition

OSNR (dB)	***Measured BER***
4	1.175e-5
6	3.201e-7
8	3.406e-9
10	1.043e-12

Table 4.2 BER Measured Before PMD Compensation

	DGD (ps)				
OSNR (dB)	***10***	***20***	***30***	***40***	***50***
4	1.288e-5	1.448e-5	1.933e-5	2.773e-5	-
6	3.295e-7	3.722e-7	5.346e-7	8.905e-7	-
8	3.571e-9	4.389e-9	6.714e-9	1.424e-9	-
10	2.434e-12	1.913e-12	8.694e-12	1.374e-11	4.535e-10

Table 4.3 BER Measured After PMD Compensation

	DGD (ps)				
OSNR (dB)	***10***	***20***	***30***	***40***	***50***
4	1.71e-5	1.096e-5	1.221e-5	1.9e-5	-
6	3.13e-7	2.971e-7	7.297e-7	3.81e-7	-
8	4.616e-9	4.716e-9	2.109e-9	4.802e-9	-
10	5.043e-12	3.819e-12	1.739e-12	4.656e-12	8.623e-11

4.4.3 Discussion and conclusion

The BER at OSNR of 8, 6 and 4 dB were too high, even at 0 ps DGD. This implies that the OSNR posed a much greater problem than PMD. Therefore, it was decided to consider PMD effects at ONSR of 10 dB and higher only.

At a 10 dB OSNR, the results clearly show that for emulated DGD values of 30, 40 and 50 ps, the BER has improved after PMD compensation. However, for emulated DGD of 10 and 20 ps, the BER has slightly worsened after compensation. This worsening in BER is believed to be due to the following reasons. First, at 10 ps and 20 ps, the effect of PMD is probably not that pronounced for OC-192 data rate. This therefore causes only a marginal reduction in the DOP and so there is a lot more ambiguity presented before the compensation system when it tries to perform the compensation. As the DGD is increased, the DOP decreases markedly, thereby removing the ambiguity. Second, for all the above tests, the compensator started it's compensation cycle with an initially assumed DGD of 25 ps. The belief is that, if the starting DGD was set closer to 10 ps and 20 ps (say at 15 ps), the compensation performance would be better.

In conclusion, it can be stated with confidence that the PMD compensator will perform good compensation of PMD at 10 dB or higher of received OSNR.

4.5 Field trial of the adaptive PMD compensation system on an underground fiber-optic link

4.5.1 Description of the set-up for the field trial

The set-up for the field trial is provided on the following page (figure 4.3). The field-trial of the adaptive PMD compensation system was performed on a buried single-mode fiber (SMF) link. The link was a concatenation of more than one span of fiber. The total length of the link was nearly 95 km.

The Agilent™ transmission test set (J2127A) was used for transmitting a pseudo-random bit sequence (PRBS, 2^{23}-1) at an OC-192 data rate. The wavelength emitted at this data rate is 1534 nm. The test set was also used for BER measurement.

The polarization controller (General Photonics™ Polarite II) was used for performing polarization scrambling. All four axes of the controller were operated. The frequencies of the driving voltages for the four axes were distributed between 80Hz and 90 Hz.

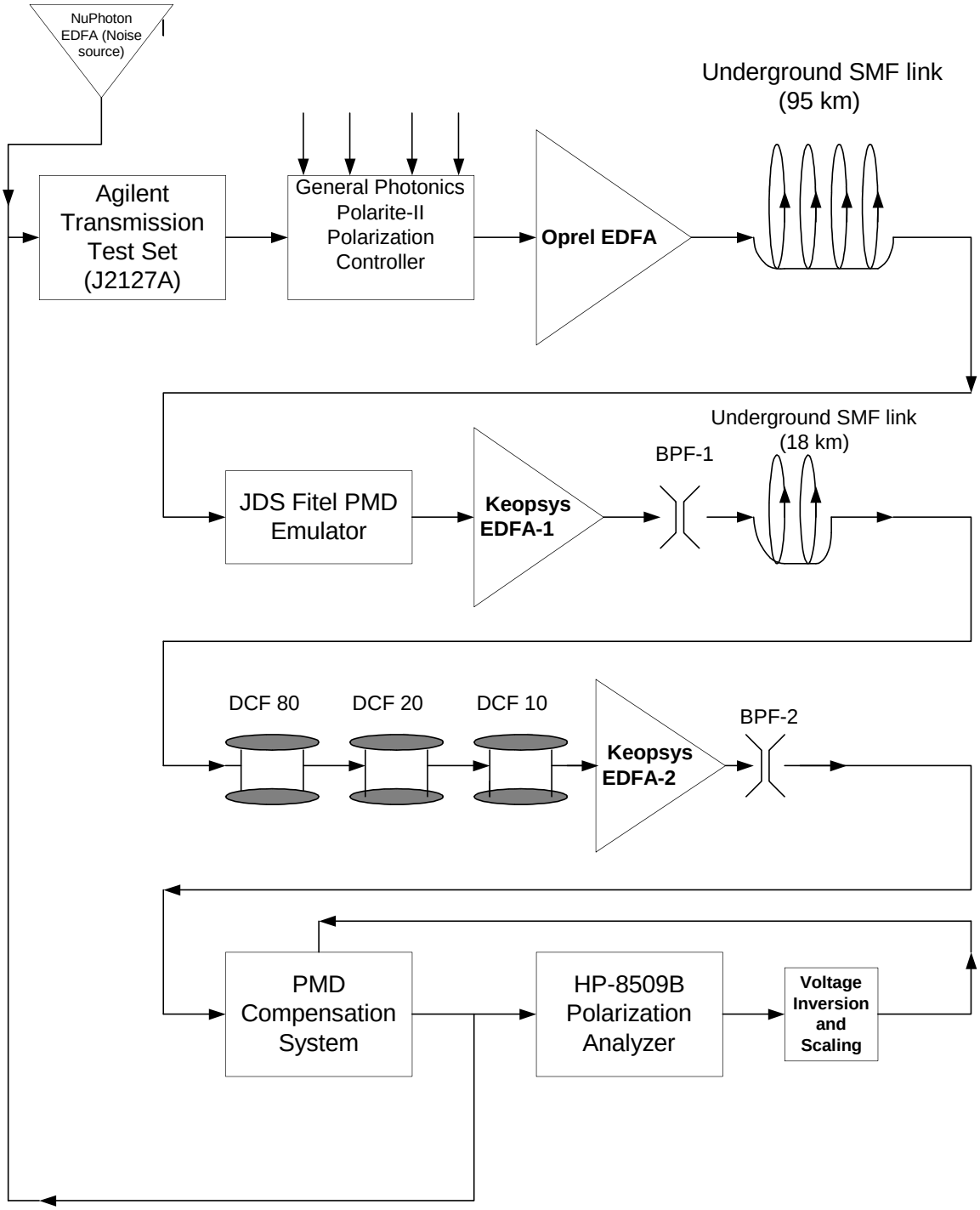

Figure 4.3 Field trial of the adaptive PMD compensation system

The Oprel™ EDFA was used as a post-amplifier. Keopsys™ EDFA-1 (with maximum output power of 27 dBm) was used after the 95 km link. Keopsys™ EDFA-2 (with maximum output power of 25 dBm) was used after the dispersion-compensating fiber (DCF) spools. The NuPhoton™ EDFA was used as a noise source and so was placed right before the BER measurement device. It's pump power was adjusted to induce a small number of bit errors and thus hasten the BER measurement process. The JDS Fitel™ PMD emulator was used to vary the DGD levels. Two tunable band-pass filters (BPF-1 and BPF-2) were required to block excessive ASE noise.

Three different Lucent™ DCF spools were used in the set-up. They were: DK-10 (-164 ps/nm), DK-20 (-335 ps/nm) and DK-80 (-1390 ps/nm). The additional 18 km of buried SMF was required for chromatic dispersion management (see section 4.5.2).

The PMD compensation system and the HP-8509B (along with the voltage inversion and scaling circuit) completed the set-up for the field trial.

4.5.2 Chromatic dispersion management* and power budget calculation

Chromatic dispersion of the 95 km link was found to be nearly 1600 ps/nm at 1550 nm and nearly 1550 ps/nm at 1534 nm. The maximum tolerable dispersion at 10 Gb/s is 1000 ps/nm [26]. Therefore, chromatic dispersion

* Adapted from the chromatic dispersion measurement and compensation performed by Ashvini Ganesh

compensation was required. To compensate for chromatic dispersion using the available dispersion-compensating fiber (DCF) fiber spools, an additional span of SMF, about 18 km long, was included. The effective chromatic dispersion was reduced to 17.6 ps/nm, at 1550 nm and nearly -10 ps/nm at 1534 nm.

Power budget calculation was performed before operating the set-up. Since the attenuation through the 95 km link was rather high (nearly 40 dB at 1550 nm), steps were taken to prevent excessive ASE noise accumulation in the set-up. First, an analytical calculation was performed to find an approximate value of the optical power that would be required at a point immediately after the 95 km link, in order to have the BER equal to 10^{-12}. The formula used for calculation and the assumptions made are provided below.

$$Q^2 \approx \frac{P_i}{4n_{sp}hfB_e} \tag{4.1}$$

The value of Q was fixed at 7 (for a BER of 10^{-12}). P_i, the optical power required at the receiver in order to obtain this BER is the quantity to be calculated. n_{sp} is the spontaneous emission factor for the Oprel™ EDFA (n_{sp} was found to be 1.581 using the following relationship: $n_{sp} = \frac{F}{2}$, where F, the noise figure of the EDFA was taken as 5 dB). B_e, the electrical bandwidth at the receiver was assumed to be 7.5 GHz (75% of the data-rate of 10 Gb/s).

The values of Planck's constant, 'h' ($6.625\times10^{-34}\,Js$) and the optical frequency (193.548 THz at 1550nm or 195.567 THz at 1534 nm) were applied.

The value of P_i was found to be -35.25 dBm (at 1550 nm) and -35.30 (at 1534 nm). Thus, it was found that a signal power level of at least -35.30 dBm would be required at the point after the 95 km link, in order to ensure a BER of 10^{-12} at this point.

A power level of 5 dBm at the input of the link would satisfy this requirement (since the loss of the link is 40 dB). However, it was decided to fix the power level at the input of the link to be equal to 15 dBm. This was for two reasons. First, the calculation presented above has assumed the noise figure F to be equal to 5 dB, which is considered very good. Practically, the noise figure value would be more than 5 dB, therefore, causing a requirement for a higher P_i. Second, in order to reduce the gain requirement from the other EDFAs used in the set-up, it was suggested that a high power be input to the link. As the number of channels used was only one, the non-linear effects of the high power of 15 dBm were expected to be restricted to self-phase modulation alone.

Figure 4.4 shows the power levels at different points in the set-up. The gains of the EDFAs are also indicated.

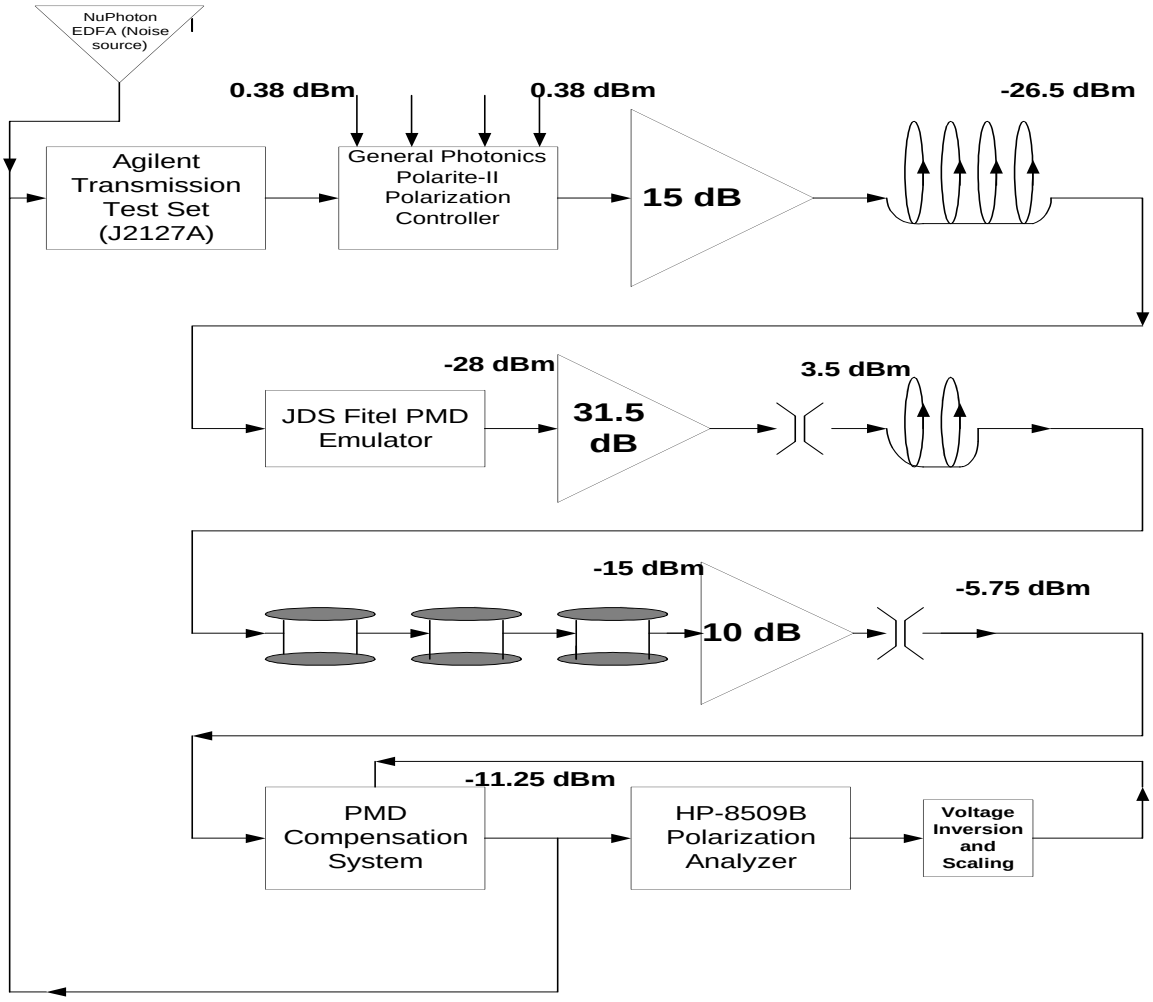

Figure 4.4 Optical power levels in the set-up

4.5.3 Tests conducted

Several tests were conducted using the above set-up. They included performance tests on the PMD compensator and tests to verify the efficacy of multi-axis polarization scrambling and various scrambling frequencies. During all the tests, initially, the BER was measured after emulating a certain amount of DGD. The PMD compensator was allowed to run. After the PMD compensator completed all it's searches, further execution of the algorithm was stopped and the post-compensation BER was measured. Several trials were conducted for one value of DGD. Similarly, the tests were repeated with different levels of emulated DGD.

The first test to be performed using the above set-up was related to the number of axes of polarization scrambling. The General Photonics™ Polarite II is a four-axis polarization controller, which can be used as a polarization scrambler. The aim of the test was to find out if there was any variation in the PMD compensation performance with change in the number of axes of polarization scrambling. The test was performed with one-axis and four-axis scrambling. The performance of the PMD compensator was expected to vary (if at all) between these two cases of scrambling axes only. The cases of two-axis and three-axis scrambling were expected to yield results similar to the four-axis scrambling case. Therefore, the number of scrambling axes was kept at one and four and the compensator's performances (defined primarily by the post-compensation BER) were compared. Initially, the BER with 0 ps of

emulated DGD was measured. Then, 30 ps of DGD was emulated in the PMD emulator and the resulting BER was measured. The post-compensation BER was compared with the above two BER values, to assess the quality of PMD compensation.

A follow-up test to the above test was performed to find out the maximum DGD that the PMD compensator could compensate satisfactorily. Single-axis scrambling was used during these tests (see section 4.3.5-A for the reason why single-axis scrambling was chosen). Starting from 35 ps, the emulated DGD was increased in steps of 5 ps and the post-compensation BER was measured for each case. The level of DGD at which the post-compensation BER had not significantly improved was found out from the compensation trials. In this manner, the maximum DGD that the PMD compensator could compensate for could be determined. To maintain consistency during the test, the starting DGD (DGD assumed by the compensator before the start of it's search processes) was modified as the DGD level was increased. For example, the starting DGD values were set at 25 ps, 30 ps and 35 ps respectively for emulated DGD values of 30 ps, 35 ps and 40 ps.

The third test that was conducted using the above set-up was related to the polarization scrambling frequency. The aim of this test was to verify the importance of choosing an optimum scrambling frequency (which is higher than the sampling frequency of the compensator and yet much lower than the

sampling frequency of the DOP measuring device). A DGD of 30 ps was emulated using the PMD emulator. Single-axis scrambling was employed for all the measurements during this test. The scrambling frequency was varied from as low as 5 Hz to as high as 1.3 kHz and the post-compensation performance was noted for each frequency setting. For scrambling frequencies between 5 Hz and 100 Hz, the PMD compensator's sampling frequency was fixed at 50 Hz. For all scrambling frequencies greater than 100 Hz, the PMD compensator's sampling frequency was 100 Hz.

The results obtained from all the above tests and the conclusions drawn have been provided in sections 4.3.5 and 4.3.6 respectively.

4.5.4 Results obtained and conclusions

A. Number of axes used for polarization scrambling versus PMD compensation performance

Table 4.4 Measured BER for emulated DGD of 0 ps and 30 ps

Emulated DGD (ps)	Measured BER
0	6.26e-12
30	3.085e-11

Table 4.5 Compensation performance with 4-axis polarization scrambling (emulated DGD=30 ps)

Trial	Compensated DGD (ps)	Measured BER
1	26	3.826e-12
2	24	2.426e-12

Table 4.6 Compensation performance with 1-axis scrambling (emulated DGD=30 ps)

Trial	Compensated DGD (ps)	Measured BER*
1	37	2.773e-12
2	24	4.159e-12

* SOP before the PMD emulator adjusted during BER measurement

From the results obtained, it was clear that the number of axes employed for polarization scrambling did not significantly impact the PMD compensator's performance. To verify this finding, an additional test was carried out. A paddle-type polarization controller was introduced right before the PMD emulator. When the post-compensation BER measurement for the 1-axis scrambling case was taking place, the state of polarization (SOP) before the PMD emulator was varied, using the paddle-type polarization controller. If 1-axis scrambling had not been an optimal solution, this variation in the SOP would have caused a noticeable increase in the number of bit errors. However, there was no such occurrence. Therefore, it was concluded that the PMD

compensator's performance is independent of the number of polarization scrambling axes.

B. Maximum DGD that can be compensated for by the PMD compensator

Table 4.7 Measured BER after PMD compensation for different values of emulated DGD (BER with emulated DGD of 0 ps was 6.26e-12)

Emulated DGD (ps)	**Compensated DGD (ps)**	**Measured BER**
30	i) 37	2.773e-12
	ii) 24	4.159e-12
35	i) 34	4.521e-12
	ii) 24	5.495e-11
40	i) 18	2.713e-11
	ii) 20	7.582e-11
	iii) 41	4.506e-11

The results show that the PMD compensator is capable of compensating for 35 ps of DGD in a satisfactory manner, even though one of the two trials yielded a high BER. However, when 40 ps of DGD were emulated, the post-compensation BER during all the three trials were relatively high. Based on

these results, it was concluded that the PMD compensator is capable of compensating for a maximum of about 40 ps of DGD.

C. Polarization scrambling frequency versus PMD compensation performance

Table 4.8a Measured BER after PMD compensation with different frequencies of polarization scrambling (emulated DGD=30 ps; PMD compensator sampling frequency of 50 Hz; BER with 0 ps of emulated DGD was 6.26e-12)

Scrambling frequency (Hz)	Compensated DGD (ps)	Measured BER
5	26	2.052e-11
10	44	4.571e-10
20	35	1.148e-11
50	15	2.156e-11
80	35	2.087e-12
100	36	3.826e-12

Table 4.8b Measured BER after PMD compensation with different frequencies of polarization scrambling (emulated DGD=30 ps; PMD compensator sampling frequency of 100 Hz; BER with 0 ps of emulated DGD was ≈ 10^{-13})

Scrambling frequency (Hz)	**Compensated DGD (ps)**	**Measured BER**	**Comments**
200	26	6.608e-12	Lengthy tracking
400	36	3.3e-13	Lengthy tracking
700	36	1.009e-11	_
1200	19	2.504e-11	Lengthy tracking
1300	25	1.461e-11	Lengthy tracking

The results shown in tables 4.8a and 4.8b show the importance of choosing carefully the scrambling frequency. In the first case (Table 4.8a), the scrambling frequencies of 5, 10, 20 and 50 Hz did not yield satisfactory BER values even after PMD compensation. That was because they were all less than or equal to the PMD compensator's sampling frequency of 50 Hz. In order for the scrambling to have it's desired effect, the compensator should take samples representing different SOP before the link/PMD emulator.

Whereas, low scrambling frequencies do not meet this condition, scrambling frequencies greater than the compensator's sampling frequency do. The PMD compensation performance with scrambling frequencies higher than 50 Hz (viz. at 80 Hz and 100 Hz) were significantly better.

In the second case (table 4.8b), the PMD compensation performance degrades as the scrambling frequency is increased. Higher frequency scrambling causes the SOP to change too rapidly, and thereby causes the SOP to change even within a DOP measurement sampling duration. This not only increases the ambiguity in the DOP measurement process, but also causes the resulting DOP signal used by the PMD compensator to fluctuate over a large range of values. Overall, the PMD compensation performance is severely degraded. The comment "lengthy tracking" indicates that the PMD compensation tracking was very lengthy or unending during these cases. Since the monitor signal fluctuated over a wide range, the threshold monitor voltage is easily breached, thereby triggering repeated tracking of the PSPs and DGD.

Based on these results, it was concluded that to perform reliable, repeatable PMD compensation in a reasonably short time, the scrambling frequencies should range between 80 Hz and 100 Hz.

5. SUMMARY, CONCLUSIONS AND SCOPE FOR FUTURE WORK

5.1 Summary

This work focused on the research on adaptive PMD compensation conducted in the lightwave communication systems laboratory at the University of Kansas.

An introduction to PMD was provided. The causes of PMD and the role of birefringence were described in detail. The characterization of PMD using the differential group delay (DGD) concept and the principal states of polarization (PSP) model was explained. The effects of PMD, especially on digital optical communication systems (where PMD manifests as inter-symbol interference or ISI) were described, following which the need for compensating for PMD at 10 Gb/s and higher data rates was discussed.

The second chapter provided an overview of the existing PMD mitigation strategies. Their relative advantages and disadvantages were also mentioned. Optical PMD compensation strategies and electronic PMD mitigation techniques were individually taken-up and described. In addition to PMD compensation, steps to mitigate or overcome PMD, such as the use of PMD resistant modulation formats, were also described.

The third chapter focused entirely on the adaptive PMD compensation system developed in the University of Kansas. The concept development, the early implementation and the enhancements that took place over the years were summarized. The need for switching from an RF tones based PMD monitoring technique to one based on the degree of polarization (DOP) of the received signal was explained. The steps in the PMD compensation algorithm, in it's present version, were given in the form of a flow-chart. A detailed description of the components that make-up the PMD compensator (viz. the polarization controller and the variable delay line) and the control signals that they receive, was provided.

The second half of chapter three dealt with polarization scrambling and it's application in PMD compensation. When the state of polarization (SOP) of the optical signal is subjected to polarization scrambling (a continuous change of the SOP), before it is transmitted into the fiber-link, the optical power is effectively equally distributed between the two PSPs of the fiber-link. This condition will enable the PMD compensation system to reliably estimate the output PSPs of the fiber-link and also the DGD. Polarization scrambling can be performed using several methods. A lithium-niobate device was initially used, which could perform one-axis scrambling (which produces a great circle on the Poincare sphere). Later, a multi-axis, fiber-squeezer type polarization-controller was used for polarization scrambling. The fiber-squeezer type device can perform multi-axis scrambling as a result of which the resulting

SOP can change over all points on the Poincare sphere (full coverage on the Poincare sphere and not just one great circle).

Chapter four described the performance tests conducted on the adaptive PMD compensation system. The operating speed of the PMD compensation (time required for one complete cycle of searches) is nearly 100 s. The optimum polarization scrambling frequency range was found through experimental studies. The scrambling frequency must be higher than the sampling rate of the PMD compensation system, but much lower than the sampling speed of the DOP measurement device. The presently used range of scrambling frequencies is from 80 Hz to 100 Hz.

Optical signal to noise ratio (OSNR) tests were conducted using the PMD compensation system to assess it's performance when used in multi-span, amplified, lightwave communication systems. The performance of the PMD compensation system was found to be good at the OSNR value of 10 dB. Below 10 dB of OSNR, noise posed a greater problem than PMD.

The fiber-squeezer type, multi-axis polarization controller facilitated tests to compare the effects of single-axis scrambling versus multi-axis scrambling. The experimental results showed that the performance of the PMD compensation system was independent of the number of axes used during polarization scrambling.

Tests were performed (at 10 Gb/s data rate) to find the upper limit of DGD that the PMD compensation system can satisfactorily compensate. Based on the improvement in post-compensation bit-error rate (BER), it was found that the PMD compensation system could compensate for a maximum of 40 ps of DGD. However, the improvement in the BER is not as good at 40 ps of DGD as it is at 35 ps of DGD.

Finally, a test to demonstrate the importance of polarization scrambling frequency was performed. Single-axis polarization scrambling was adopted and the scrambling frequency was varied from a low value (5 Hz) to a high value (1.3 kHz). As expected, the PMD compensation performance was best for the scrambling frequencies of 80 Hz and 100 Hz (which are both higher than the PMD compensation system's sampling frequency and much lower than the DOP measurement sampling frequency).

5.2 Conclusions

An adaptive PMD compensation system was modified into a robust and bit-rate independent one. The PMD monitoring mechanism was significantly altered. The present mechanism is based on the DOP of the received signal. The problem of polarization-dependent loss (PDL) in the PMD compensation system was resolved.

An optimum polarization scrambling frequency range was experimentally determined so as to cause minimal interference to the DOP measurement (and therefore to the PMD compensation performance).

Through experiments, it was found that the PMD compensation system would perform satisfactory compensation at 10 dB of optical signal to noise ratio (OSNR) and higher. Also, it was found that below 10 dB of OSNR, noise was a greater problem than PMD.

A field trial of the adaptive PMD compensation system was successfully conducted on an underground fiber-optic link spanning 95 km. The maximum limit of DGD that the PMD compensator could compensate was found to be about 40 ps.

By performing tests using a multi-axis polarization controller, it was found that the PMD compensation performance was independent of the number of axes of scrambling. Additional performance tests on the PMD compensation system reaffirmed the importance of choosing the right scrambling frequency.

5.3 Scope for future work

The PMD monitoring mechanism based on DOP is here to stay. Therefore, in place of the HP 8509B polarization analyzer, (which is more of a laboratory instrument than a device suitable for PMD compensation system applications) a compact polarimeter which can perform high speed DOP measurement and provide instantaneous DOP data, can be used.

Following that will be the need to test the PMD compensation system's performance at 40 Gb/s data rate. The bit-rate independence of the PMD compensation system will make the transition to the realm of 40 Gb/s a rather simple one.

Next will be the issue of higher-order PMD. At 40 Gb/s, the higher-order PMD (especially second-order PMD) effects will not be negligible. The performance of the PMD compensator can be evaluated in the higher-order PMD environment also.

Finally, the PMD compensation system's performance can be evaluated for other modulation formats such as RZ (return-to-zero).

References

1. Agrawal, G.P. , *Fiber optic Communication Systems*, Second Edition, John Wiley, New York, NY, 1997.

2. Poole, C.D., and J.Nagel, "Polarization effects in lightwave systems," Chapter 6, *Optical Fiber Telecommunication,* volume III A, edited by I.P.Kaminow and T.L.Koch, Academic Press, San Diego, CA, 1997.

3. Pua, H.Y., K. Peddanarappagari, B. Zhu, C. Allen, K. Demarest, and R. Hui, "An adaptive first-order polarization-mode dispersion compensation system aided by polarization scrambling: theory and demonstration," *Journal of Lightwave Technology*, 18(6), pp. 832-841, 2000.

4. Poole, C. D. and R. E. Wagner, "Phenomenological approach to polarization mode dispersion in long single-mode fibers," *Electronics Letters*, 22(19), pp. 1029-1030, 1986.

5. Kogelnik, H., R.M. Jopson and L.E.Nelson, "Polarization-Mode Dispersion," Chapter 15, *Optical Fiber Telecommunications*, volume IV B, edited by I.P.Kaminow and T.Li, Academic Press, San Diego, CA, 2002.

6. Poole, C. D. and C. R. Giles, "Polarization-dependent pulse compression and broadening due to polarization dispersion in dispersion-shifted fiber," *Optics Letters*, 13(2), pp. 155-157, 1988.

7. Poole, C. D. and T. E. Darcie, "Distortion related to polarization mode dispersion in analog lightwave systems," *Journal of Lightwave Technology*, 11(11), pp. 1749-1759, 1993.

8. Takahashi, T., T. Imai, and M. Aiki, "Automatic compensation technique for timewise fluctuating polarization mode dispersion in in-line amplifier systems," *Electronics Letters*, 30(4), pp. 348-349, 1994.

9. Kikuchi, N. and S. Sasaki, "Polarization-Mode Dispersion (PMD) detection sensitivity of degree of polarization method for PMD compensation," *Proc. ECOC'99*, Nice, France Vol. II, p. WeA1.3, pp. 8-9, 1999.

10. Kikuchi, N., "Analysis of signal degree of polarization degradation used as control signal for optical polarization mode dispersion compensation," *Journal of Lightwave Technology*, 19(4),pp. 480-486, 2001.

11. Buchali, F., S. Lanne, J.-P. Thiéry, W. Baumert and H. Bülow, "Fast eye monitor for 10 Gbit/s and its application for optical PMD compensation," *Proc. OFC'2001*, Los Angeles, CA, paper TuP5, 2001.

12. Heismann, F., D. A. Fishman, and D. L. Wilson, "Automatic compensation of first-order polarization mode dispersion in a 10 Gb/s transmission system," *Proc. ECOC 1998*, Madrid, Spain, Vol. I, pp. 529-530, 1998.

13. Rosenfeldt, H., Ch. Knothe, R. Ulrich, E. Brinkmeyer, U. Feiste, C. Schubert, J. Berger, R. Ludwig, H. G. Weber, and A. Ehrhardt, "Automatic PMD compensation at 40 Gbit/s and 80 Gbit/s using a 3-dimensional DOP evaluation for feedback," *Proc. OFC'2001*, Los Angeles, CA, Postdeadline Papers, paper PD27, 2001.

14. Karlsson. M., C. Xie, H. Sunnerud, and P.A. Andrekson, "Higher order polarization mode dispersion compensator with three degrees of freedom," *Proc. OFC'2001*, Los Angeles, CA, paper MO1, 2001.

15. Ono, T., S. Yamazaki, H. Shimizu, and K. Emura, "Polarization control method for suppressing polarization mode dispersion influence in optical transmission systems," *Journal of Lightwave Technology*, 12(5), pp. 891-898, 1994.

16. Patscher, J. and R. Eckhardt, "Component for second-order compensation of polarization mode dispersion," *Electronics Letters*, 33(13), pp. 1157-1159, 1997.

17. Shtaif, M., A. Mecozzi, M. Tur, and J.A. Nagel, "A compensator for the effects of high-order polarization mode dispersion in optical fibers," *IEEE Photonics Technology Letters*, 12(4), pp. 434-436, 2000.

18. Bülow, H., G. Thielecke, "Electronic PMD mitigation - from linear equalization to maximum-likelihood detection," *Proc. OFC'2001*, Los Angeles, CA, paper WAA3, 2001.

19. Chou, P. C., J. M. Fini, and H. A. Haus, "Demonstration of a feed-forward PMD compensation technique," *IEEE Photonic Technology Letters*, 14(2), pp. 161-163, 2002.

20. Xie, Y., Q. Yu, L.-S. Yan, O. H. Adamczyk, Z. Pan, S. Lee, A. E. Willner, and C. R. Menyuk, "Enhanced PMD mitigation using forward-error-correction coding and a first-order compensator," *Proc. OFC'2001*, Los Angeles, CA, paper WAA2, 2001.

21. Khosravani, R. and A. E. Willner, "Comparison of different modulation formats in terrestrial systems with high polarization mode dispersion," *Proc. OFC 2000*, Baltimore, paper WL5, pp. 201-203, 2000.

22. Pierre. L. and , J.-P. Thiery, "Comparison of resistance to polarization mode dispersion of NRZ and phase-shaped binary transmission formats at 10 Gbit/s," *Electronics Letters*, 33(5), pp. 402-403, 1997.

23. Kaiser, W., W. Otte, T. Wuth, and W. Rosenkranz, "Experimental verification of reduced sensitivity of optical duobinary modulation to higher order PMD," *OFC '02*, Anaheim, CA, TuI5, pp. 53-54, 2002.

24. Pua, H.Y., "First-order polarization-mode dispersion adaptive compensation system," Master's thesis, Department of Electrical Engineering and Computer Science, University of Kansas, Lawrence, KS, 1998.

25. Derickson, D., editor, *Fiber Optic Test and Measurement*, Prentice-Hall, Inc., Upper Saddle River, NJ, 1998.

26. "Dispersion Measurements of High-Speed Lightwave Systems," *http://www.educatorscorner.com/tools/lectures/slides/pdf/3_Dispersion_Measure.pdf,* Agilent Technologies.

APPENDIX A

UPDATED INTERFACE DESIGN FOR THE PMD COMPENSATION DEVICE

Juan M. Madrid
ITTC - University of Kansas
May 15, 2001

A.1 INTRODUCTION

The original design for the PMD compensation device microprocessor interface allows to control the E-TEK FPCR-1B polarization controller and the Santec ODL-620 delay line used in the compensation device. However, the polarization controller is not directly driven by the interface card, but by a special driver supplied by E-TEK. This driver takes the 4 DC voltages generated by the interface board and converts them into 4 AC voltages, which can be directly applied to the polarization controller.

The E-TEK driver is, however, a large and heavy device which cannot be easily fitted into a chassis with the rest of the PMD compensation device. Moreover, this driver has to be manually set upon startup, so it will accept the incoming DC voltages from the interface board as control signals.

These limitations motivated the redesign of the interface board, in order to include the necessary circuitry to bypass the E-TEK driver by generating control signals the polarization controller can use directly.

A.2 SIGNAL REQUIREMENTS

According to manufacturer specifications, the E-TEK polarization controller needs four independent AC voltages, one for each of its liquid crystal cells. Each one of the AC voltages must meet the following guidelines:

- Shape: Square wave, 50% duty cycle.
- Amplitude: 2 to 12 volts peak-to-peak.
- Frequency: 200 to 2000 Hz.

According to previous experiments conducted in the laboratory, the frequency of the AC signal does not have a great influence on the polarization controller behavior. Thus, the only parameter that has to be adjusted is the voltage of the signal. Each voltage controls the amount of polarization rotation each liquid crystal cell introduces into the incoming laser beam.

A.3 INTERFACE BLOCK DIAGRAM

The following diagram shows the interface board's main blocks, along with the connections between them.

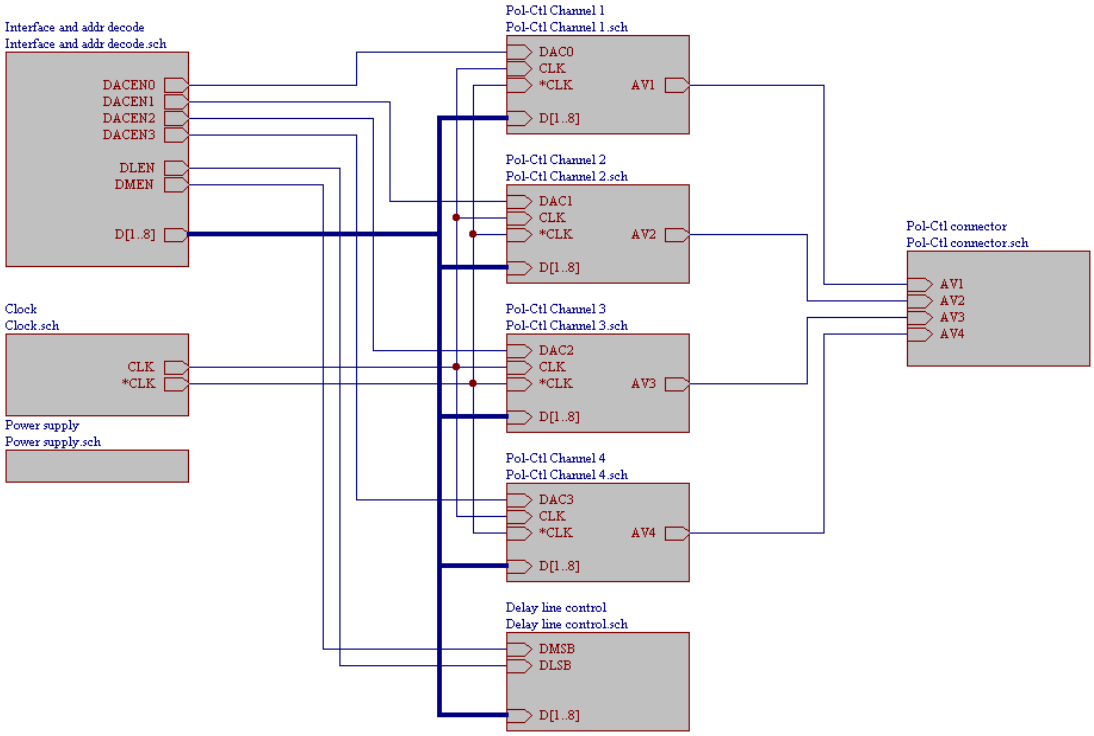

Figure A.1 Interface board block diagram

The main blocks of this design are:

- Microprocessor interface and address decoding block: Processes signals from the microprocessor's control bus, in order to route data to the adequate output port.
- Clock: Generates the reference signal the polarization controller channels will use to synthesize their AC signals.
- Polarization controller channel (PC channel): This output port gets a 8-bit value from the microprocessor and generates a variable amplitude AC signal, which is delivered to the polarization controller. The board features 4 independent PC channels, one for each polarization controller cell.

- Delay line control: This output port reads a 11-bit value from the data bus and sends it to the delay line. It also handles the "motor off" signal, which is used by the delay line to hold the program execution until the delay value is stable.

A.4 MICROPROCESSOR INTERFACE AND ADDRESS DECODER

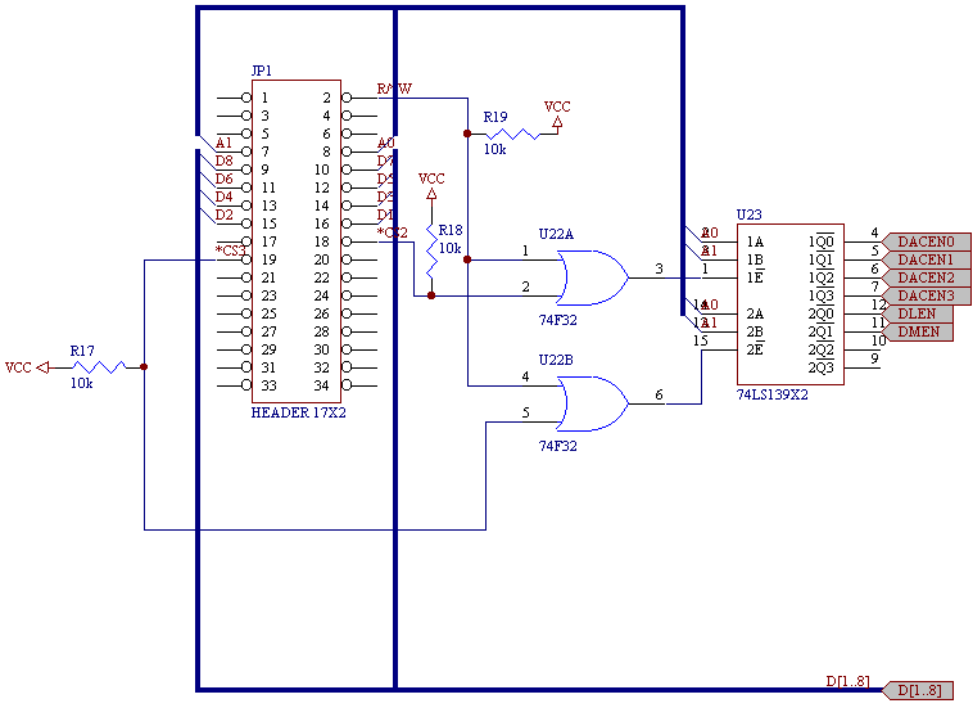

Figure A.2 Microprocessor interface and address decoder schematic diagram

The address decoder has been greatly simplified by the use of the 74LS139 integrated circuit, which features two 2-to-4 line decoders in a single chip. The truth table for the 2-to-4 decoder is shown below.

Table A.1 Truth table for 2-to-4 decoder

INPUTS			OUTPUTS			
E	**B**	**A**	**Q0**	**Q1**	**Q2**	**Q3**
1	X	X	1	1	1	1
0	0	0	0	1	1	1
0	0	1	1	0	1	1
0	1	0	1	1	0	1
0	1	1	1	1	1	0

Note: X = Don't care (0 or 1)

As stated in the design document for the previous version of the interface, the polarization controller cells are mapped in 4 consecutive

memory positions of the microprocessor memory space, starting with $4:0000 (page 4, offset 0) and ending with $4:0003 (page 4, offset 3). The chip select line CS2 is programmed to go to logical zero (low level) each time a memory position in page 4 is referenced.

Similarly, the two control bytes of the delay line are mapped in 2 consecutive memory positions, $5:0000 and $5:0001. The chip select line CS3 is programmed to go to logical zero each whenever a memory position in page 5 is referenced.

The two decoders inside the 74LS139 chip are used; one for addressing the polarization controller cell controllers, and other for addressing the delay line control section.

Whenever one of the 4 memory positions in page 4 is being written to (that is, a polarization cell voltage has been changed), control lines CS2 and R/W go to logical zero, enabling the first decoder. Depending on the memory position addressed, only one polarization controller channel is enabled at a time, as shown in the following table:

Table A.2 Control sequence of Polarization-controller channels

Memory position	Value of A1	Value of A0	Channel enabled
$4:0000	0	0	Channel 1
$4:0001	0	1	Channel 2
$4:0002	1	0	Channel 3
$4:0003	1	1	Channel 4

Similarly, when one of the two memory positions in page 5 is being written to (for a delay value change), control lines CS3 and R/W go to logical zero, enabling the second decoder. Depending on the memory position addressed, a control byte in the delay line is enabled for writing, as shown in the following table:

Table A.3 Control of delay-line

Memory position	Value of A1	Value of A0	Byte enabled
$5:0000	0	0	Low (LSB)
$5:0001	0	1	High (MSB)

A.5 CLOCK CIRCUIT

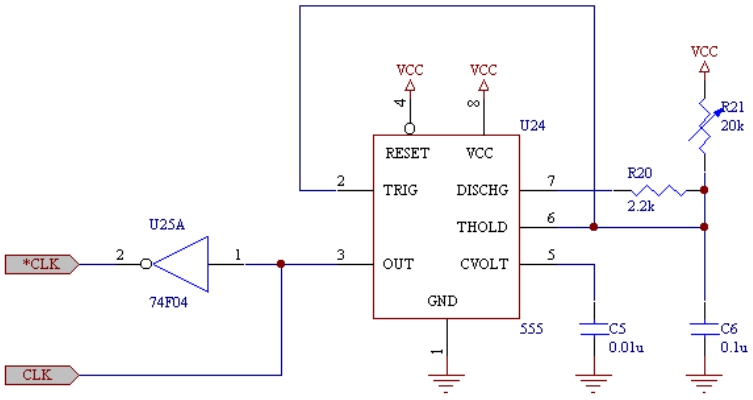

Figure A.3 Clock circuit schematic diagram

The clock circuit was designed using the LM555 timer circuit. Its design is based in the "50% duty cycle oscillator" circuit, presented in the LM555 data sheet (page 10), available from National Semiconductor (www.national.com). See the Appendix for a copy of this page.

The chosen component values yield a clock frequency of 1.5 kHz, approximately. The trimmer (R21) is used to change the square wave duty cycle during the interface board calibration.

The clock has two outputs, one normal and one inverted. Both outputs are used by the polarization controller channels.

A.6 POLARIZATION CONTROL CHANNELS

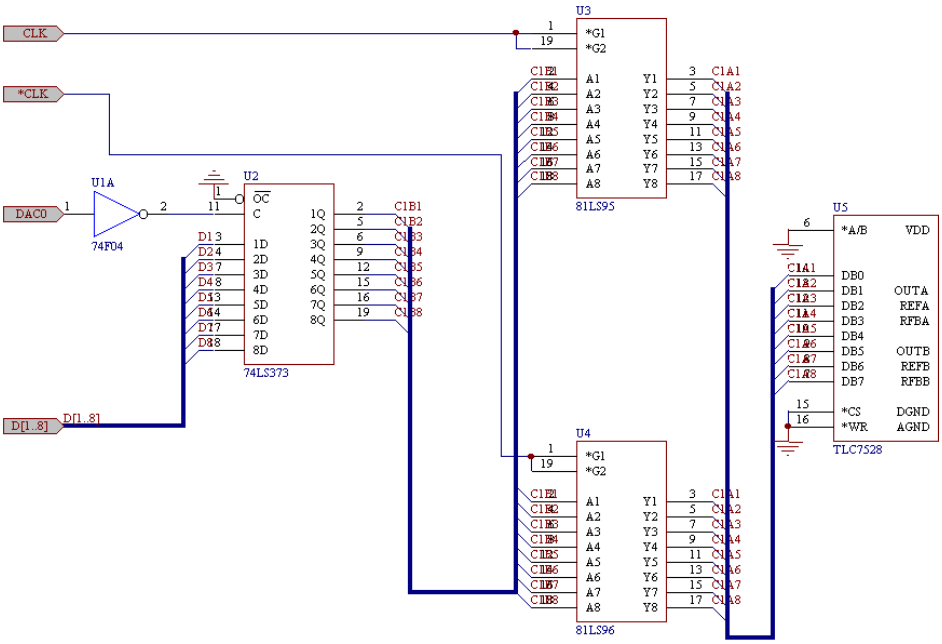

Figure A.4 Polarization control channel schematic diagram: Data latch, buffer / inverter and DAC

Each polarization controller channel is composed of four main parts:

- A data latch
- A buffer / inverter
- A Digital-to-Analog converter (DAC)
- A signal conditioning section

The data latch section uses the 74HCT373 integrated circuit (octal D-type latch), already used in the previous version of the board for the delay line data port. Whenever the latch enable signal (coming from the address decoding circuitry) goes to a logical zero, latch pin 11 receives a logical one, and the value currently present in the data bus is stored in the latch and shown at its outputs. When pin 11 returns to zero, the value in the latch is retained until the next time the latch is enabled.

The buffer / inverter section uses two chips: the DM81LS95 (a tri-state buffer) and the DM81LS96 (a tri-state inverter). The inputs of both chips are connected to the latch output, and their outputs are connected together to the DAC input. The buffer is enabled by the normal clock, and the inverter is enabled by the inverted clock (both are never enabled at the same time, to avoid shorts). Thus, for a given value at the input latch, the output of the buffer / inverter is the value of the latch and the negated value of the latch, alternatively. For example, if the value in the input latch is 0x33 (01010101), the output of the

buffer / inverter will show 0x33 and 0xAA (10101010) alternatively; the changes will occur at the same rate as the clock frequency.

The DAC section uses the TLC7528 chip (8-bit multiplying DAC) from Texas Instruments. This chip has two built-in DACs; however, only one of them (converter A) is used. This is accomplished by placing a fixed logical zero on pin 6 (A/B select). Pins 15 (Chip Select) and 16 (Write Enable) are also fixed in logical zero; this way the DAC is always watching for changes in its input.

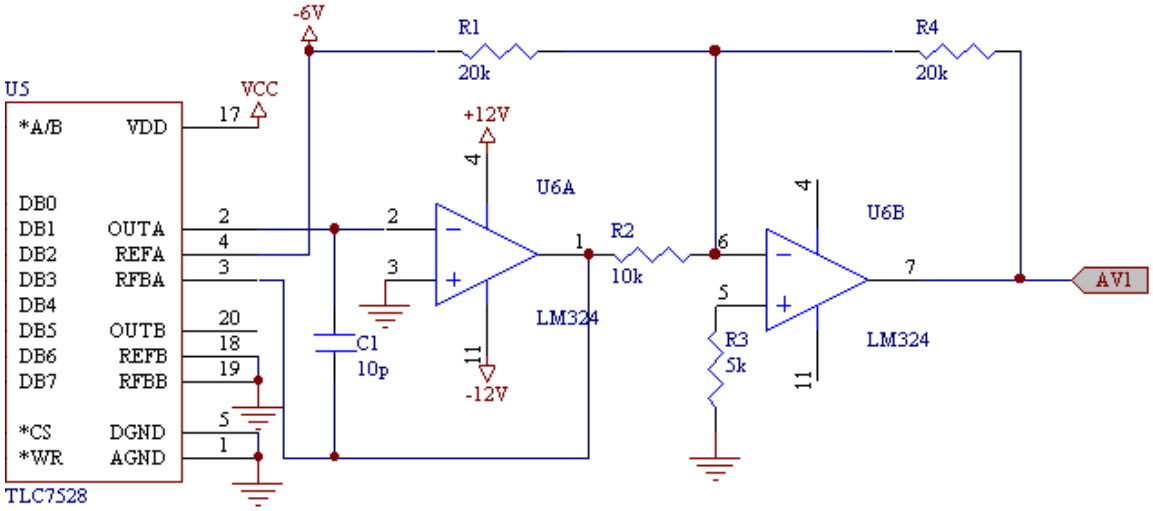

Figure A.5 Polarization control channel schematic diagram: DAC and signal conditioning section

The signal conditioning section is designed as recommended in the TLC7528 data sheet (page 8, figure 4: Bipolar operation. See the Appendix for a copy of this page). With this configuration, and a reference voltage of 6V, the maximum output voltage of the DAC is 6V (with a value of 0x00, 0000000, in the digital input) and -6V (with a value of 0xFF, 11111111, in the digital input). A value of 0x80 (1000000) will yield an output of zero volts.

The purpose of feeding normal and inverted data to the DAC at the clock frequency rate can be clearly seen now. By doing the inversion operation, the output voltage is constantly changed from a positive value to its equivalent negative value at the clock rate, effectively generating a square-wave AC signal.

If the maximum peak-to-peak voltage needs to be adjusted, the only parameter that needs to be changed is the reference voltage in the signal conditioning section. In this design, the reference voltage is -6V DC, but it can be any negative voltage up to -10V DC.

A.7 DELAY LINE CONTROL

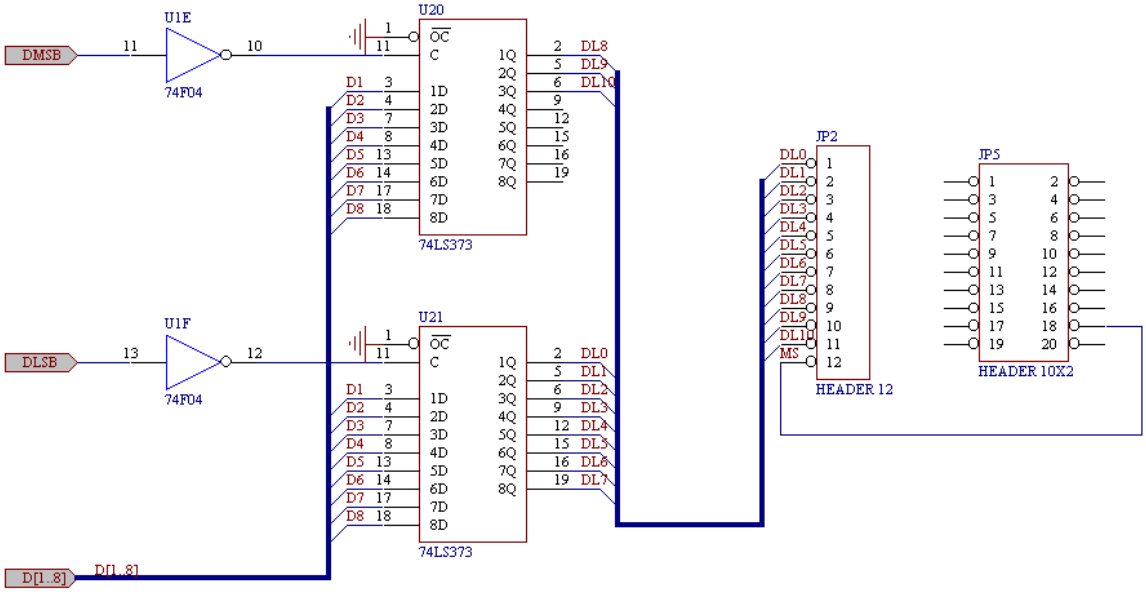

Figure A.6 Delay line control schematic diagram

Since the microprocessor data bus is 8 bits wide and the delay line interface requires 11 bits, this section uses two 74HCT373 latches. One of them stores the 8 least significant bits (D0 to D7), and the other stores the 3 more significant (D8 to D10).

The latches are enabled by the address decoding circuitry, whenever a memory position on page 5 is written to.

The delay line also features an output signal (the "motor off" signal), which goes to logical one whenever the delay line motor is stopped. To use this signal to hold the program execution until the delay line stabilizes, the signal is fed to the microprocessor as the LSB of port E, accessible through connector CN2 in the microprocessor board. Then, port E is programmed as an input, and the LSB of this port is polled whenever the delay value is changed.

A.8 POWER REQUIREMENTS

The interface board requires four voltage sources:

- +5V, for the digital circuitry (all signals are TTL-compatible)
- +12V, for the signal conditioning section of the PC channels.
- -12V, for the signal conditioning section of the PC channels.
- -6V, the reference voltage for the PC channels.

The power supply of the PMD compensation device is able to provide +5V, +15V and -15V. To get the +12V and -12V voltages, the interface board has two integrated voltage regulators. To get the -6V reference voltage, an external power conditioning board is used.

A.9 INTERFACE BOARD ASPECT – IDENTIFICATION OF FUNCTIONAL BLOCKS

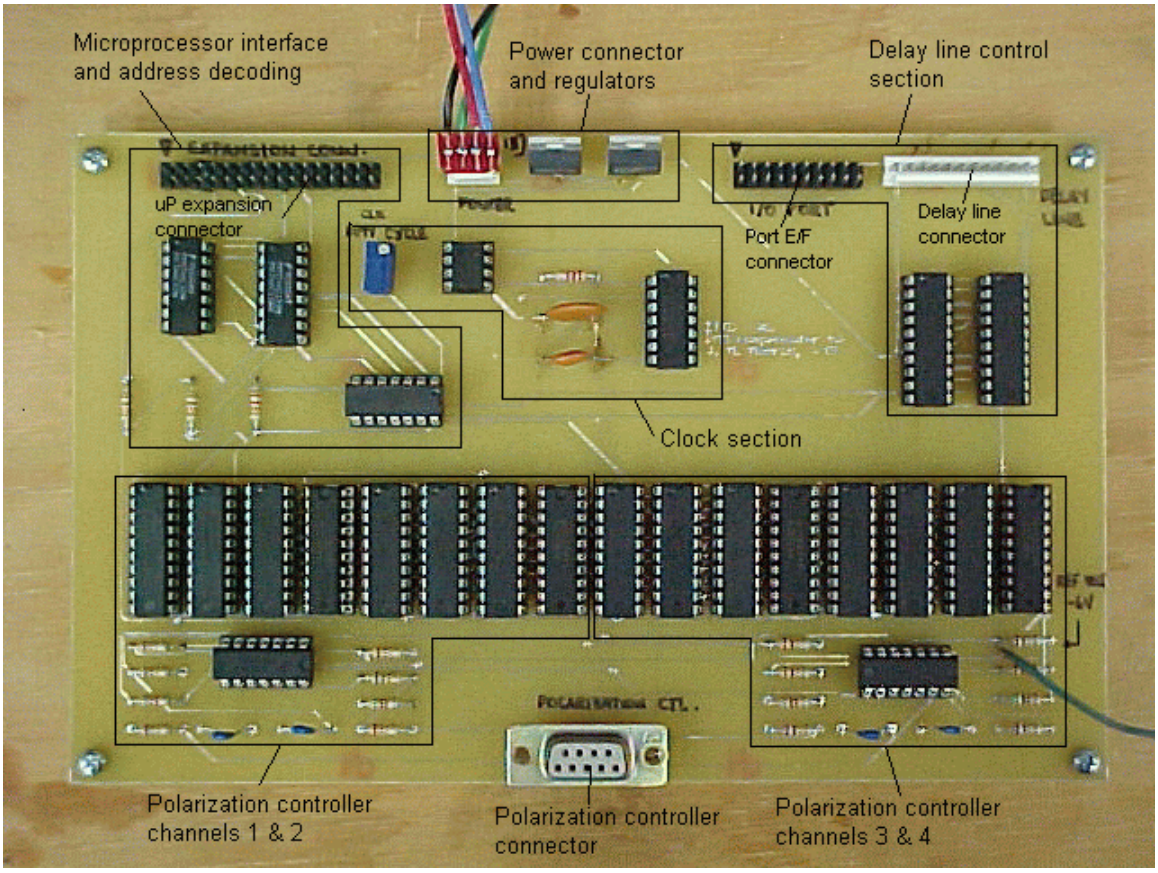

Figure A.7 Interface board

APPENDIX B

Figure B.1 is the circuit that is used for performing the voltage inversion and scaling of the degree of polarization (DOP) analog voltage that is provided by the HP-8509B. The HP-8509B provides an analog voltage equivalent of the DOP which ranges between -10 V and 0 V (0% DOP corresponds to -10 V and 100% DOP corresponds to 0 V). The circuit inverts and scales the voltages so that they range between 0 V (for 0% DOP) and 5 V (for 100% DOP).

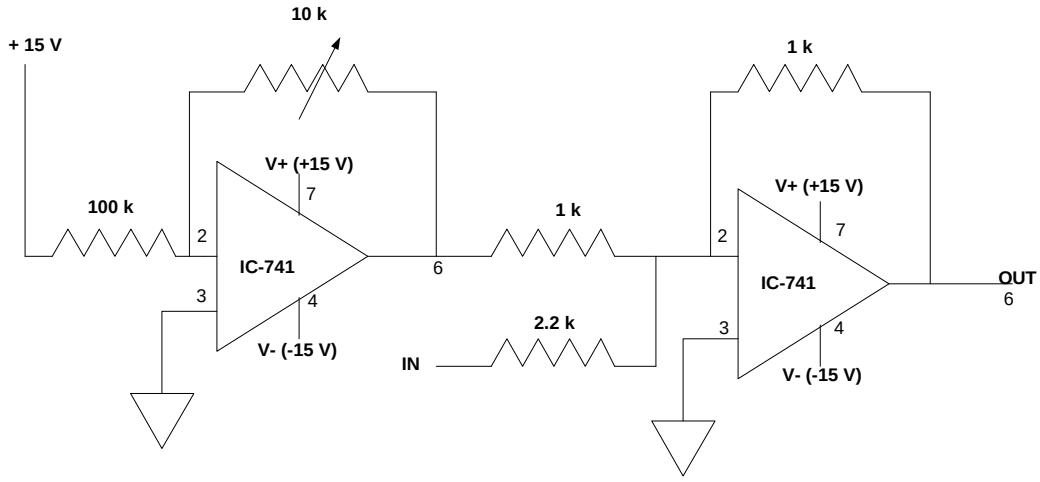

Figure B.1 Voltage inversion and scaling circuit used with the PMD compensation system